Plasmas for additive manufacturing

OLTP Seminar

See Y. Sui *et al.*, *Plasma Proc. Polym.* **17**, e20000009 (2020).

UNIVERSITY OF ILLINOIS URBANA-CHAMPAIGN

R. Mohan Sankaran
Donald Biggar Willett Professor in Engineering
Department of Nuclear, Plasma, and Radiological Engineering

Email: rmohan@illinois.edu
Website: https://speclab.npre.Illinois.edu

additive manufacturing (AM) – a process of joining materials to make objects from 3D model data, usually layer upon layer, as opposed to subtractive manufacturing technologies.

ASTM F2792-12a: Standard Terminology for Additive Manufacturing Technologies, 2013.

Subtractive vs. additive approaches to materials manufacturing

Subtractive:

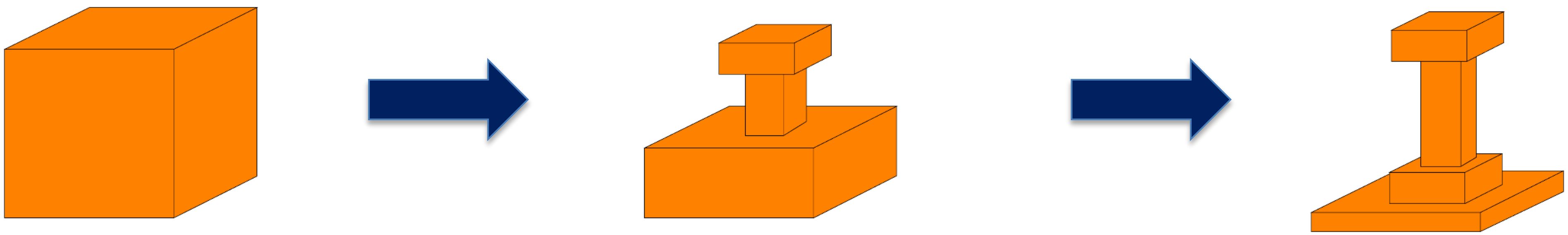

Material wasteage, relatively fast and easy, ideal for large parts

Additive:

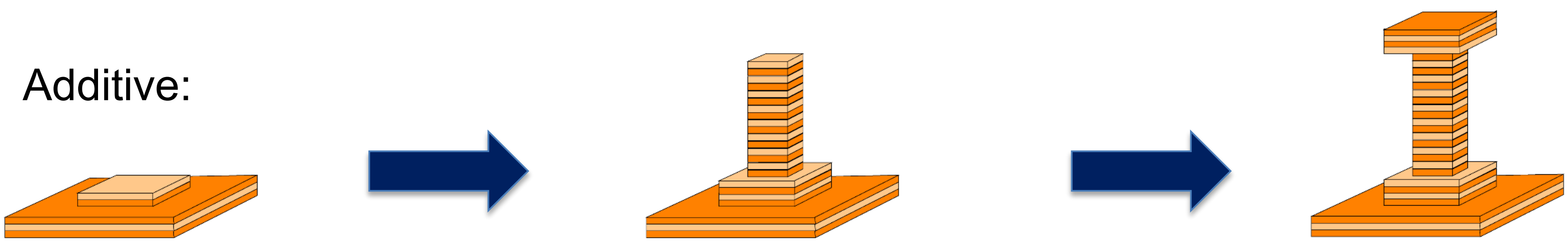

Slow and complex, enables intricate geometries, small parts

Examples of additive manufacturing

Stereolithography: Kodama, Nagoya MIRI, 1980; Hull, 3D Systems Corp., 1984

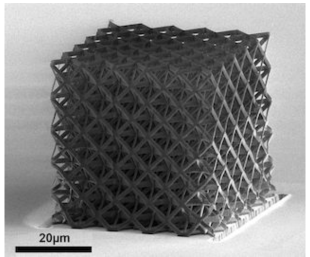

Greer, Caltech

Binder jetting: Sachs, MIT, 1993

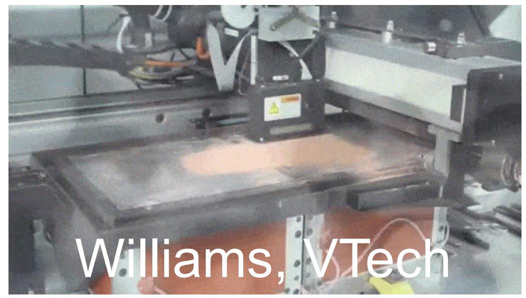

FDM patent ends, 2009

1980 1990 2000 2010

Forced deposition modeling: Crump, 1988

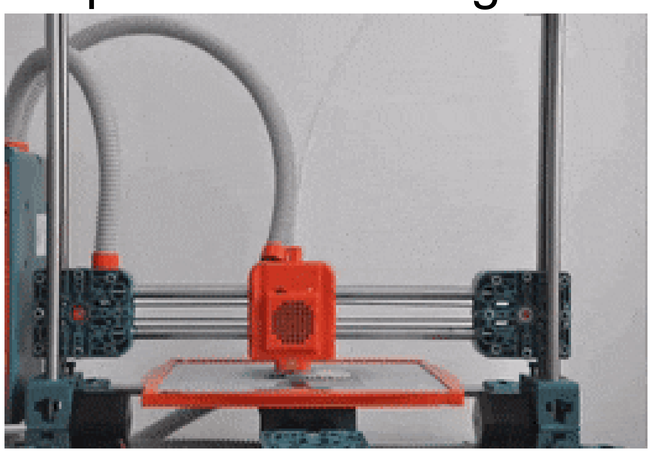

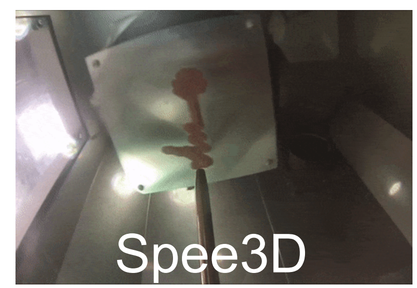

Cold spray: 2000s

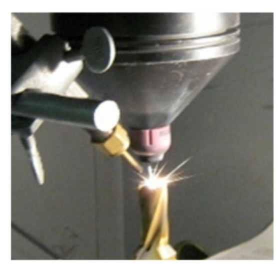

Selective laser sintering: Fraunhofer Institute, 1995

Thin film printing approaches

Screen printing
(Doctor's blade)
(Gravure printing)

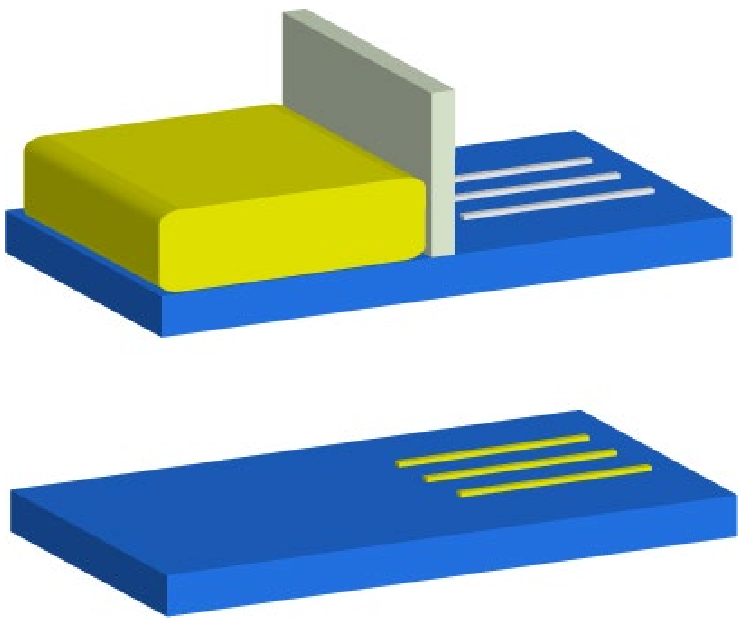

Inkjet printing
(Aerosol jet printing)

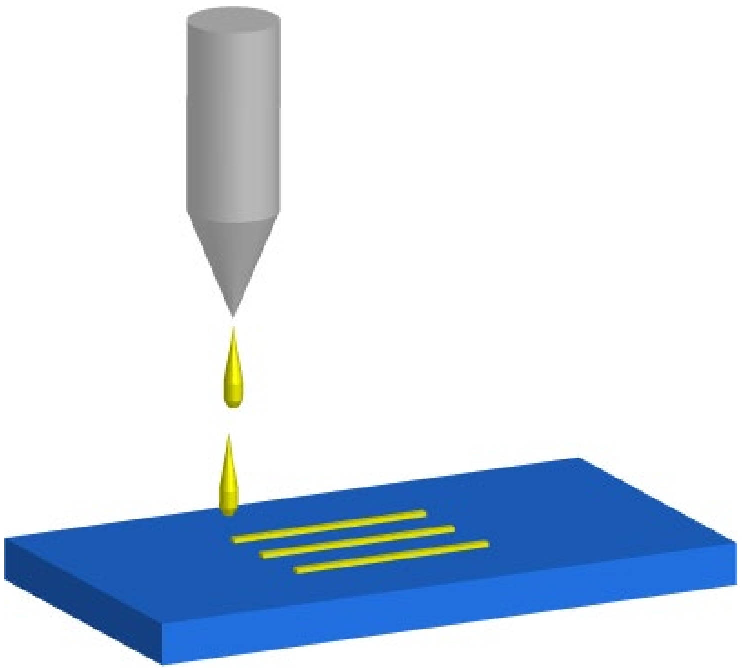

Limited to a few metals (Ag, Cu, …)

Opportunities for plasmas in additive manufacturing

PROCESSING
- Direct deposition
- Hard/Soft

NEW MATERIALS
- Metals
- Semiconductors

SURFACE TREATMENT
- Hydrophilic/phobic
- Functionalization

PLASMA
- Low-temperature
- Gas-phase
- Non-equilibrium chemistry
- Conformal

REMOVAL
- Etching/sputtering
- Corrections

MULTIPHASE
- Liquids
- Aerosols

Opportunities for plasmas in additive manufacturing

PROCESSING
- Direct deposition
- Hard/Soft

NEW MATERIALS
- Metals
- Semiconductors

SURFACE TREATMENT
- Hydrophilic/phobic
- Functionalization

PLASMA
- Low-temperature
- Gas-phase
- Non-equilibrium chemistry
- Conformal

REMOVAL
- Etching/sputtering
- Corrections

MULTIPHASE
- Liquids
- Aerosols

Potential strategies for plasma synthesis of printed structures

DIRECT WRITE

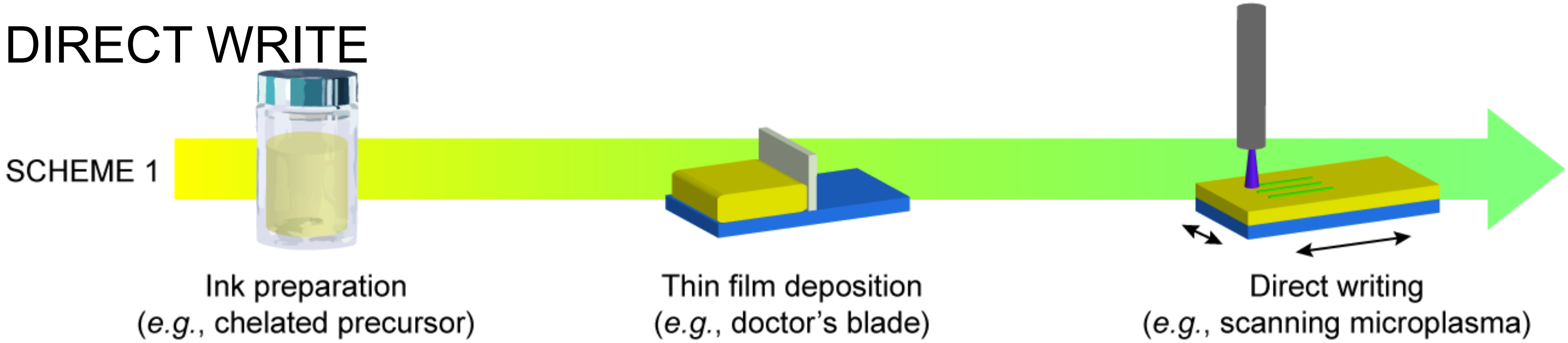

Potential strategies for plasma synthesis of printed structures

DIRECT WRITE

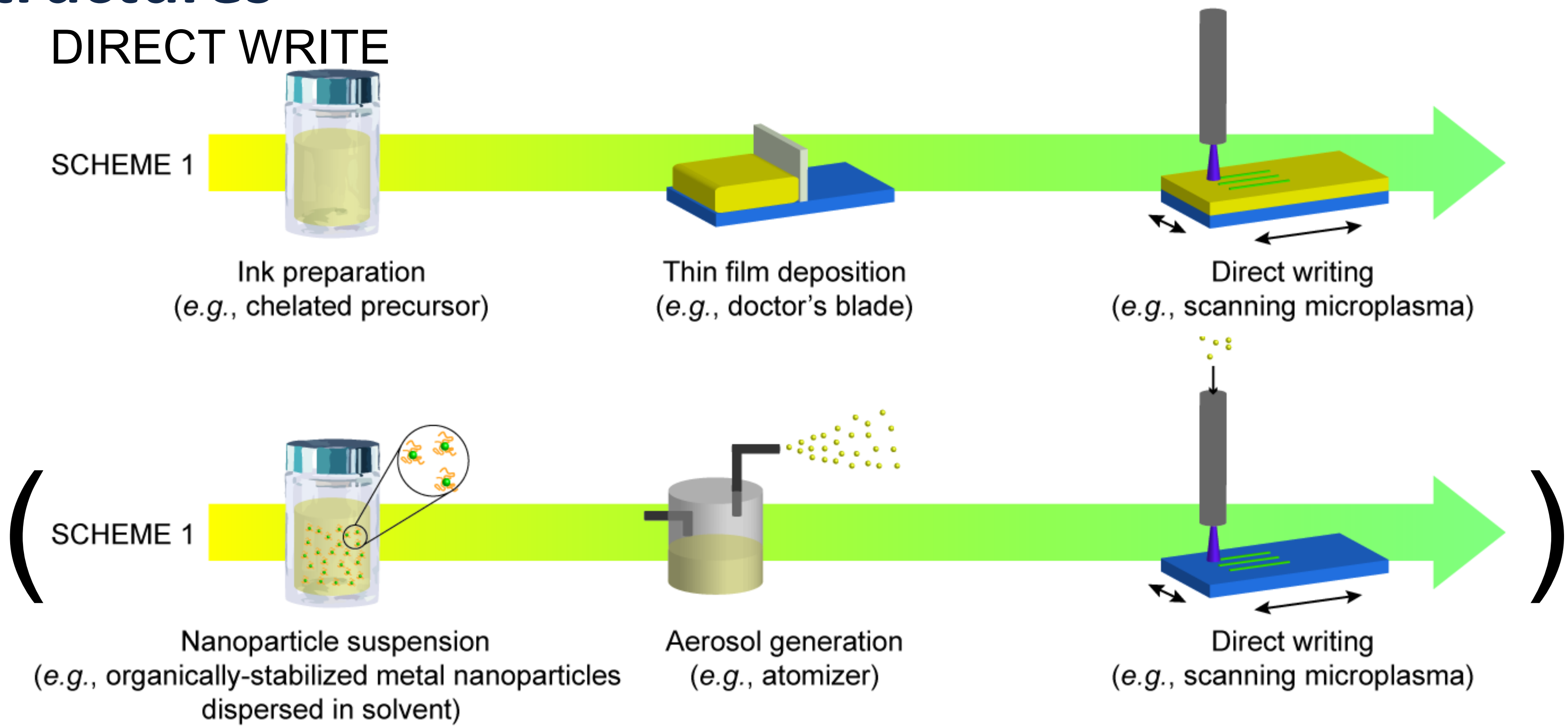

Potential strategies for plasma synthesis of printed structures

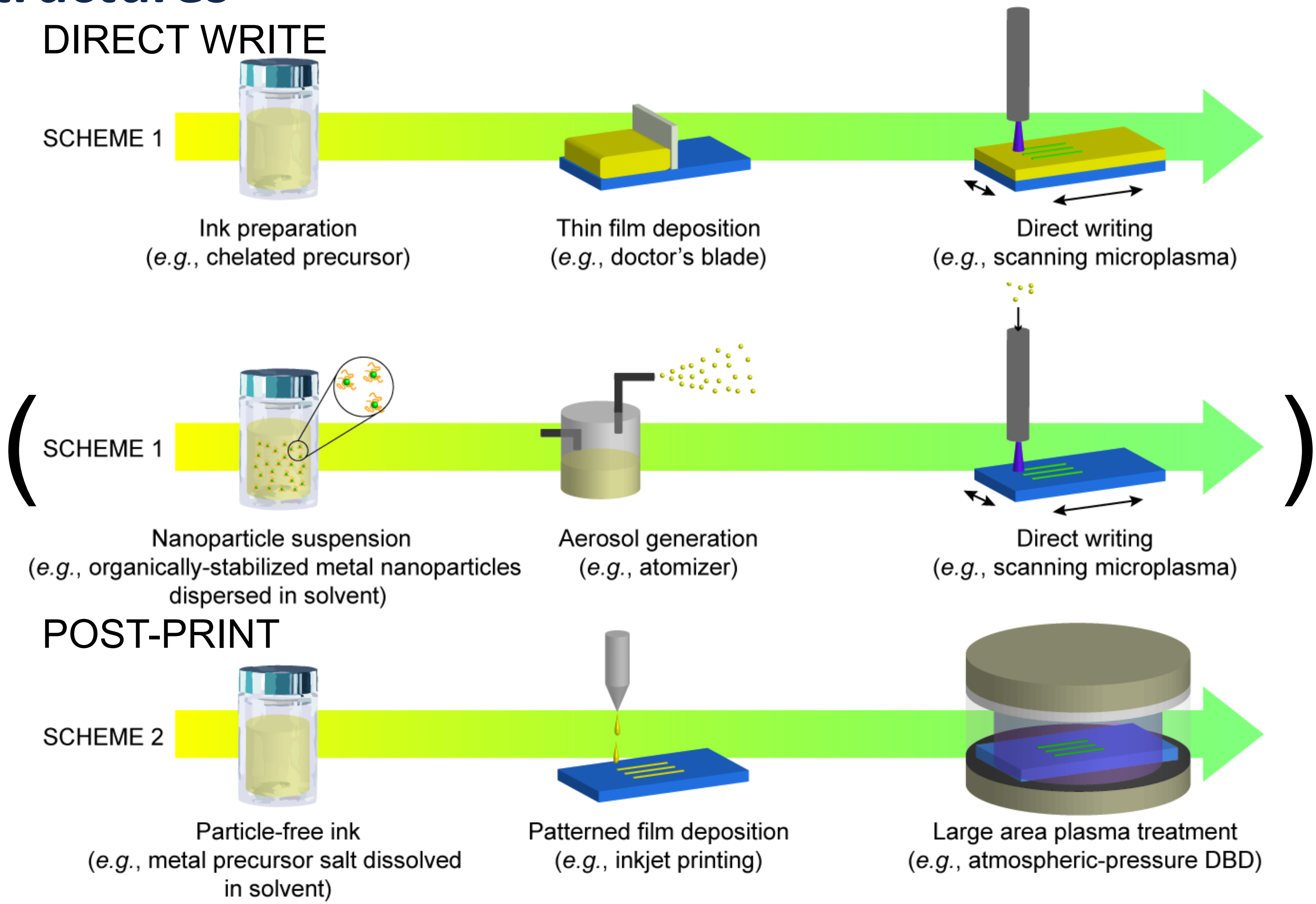

I. Direct write
   a. Nanoparticle deposition
   b. Reduction of dispersed metal salts

II. Post-print
   a. Sintering
   b. Conversion
   c. Beyond metals

I. Direct write
   a. Nanoparticle deposition
   b. Reduction of dispersed metal salts

II. Post-print
   a. Sintering
   b. Conversion
   c. Beyond metals

Synthesis of nanoparticles from liquid aerosol droplets

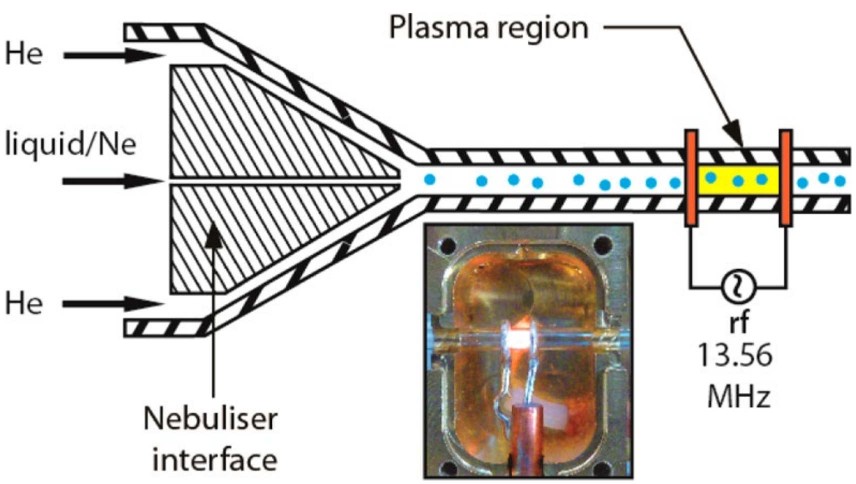

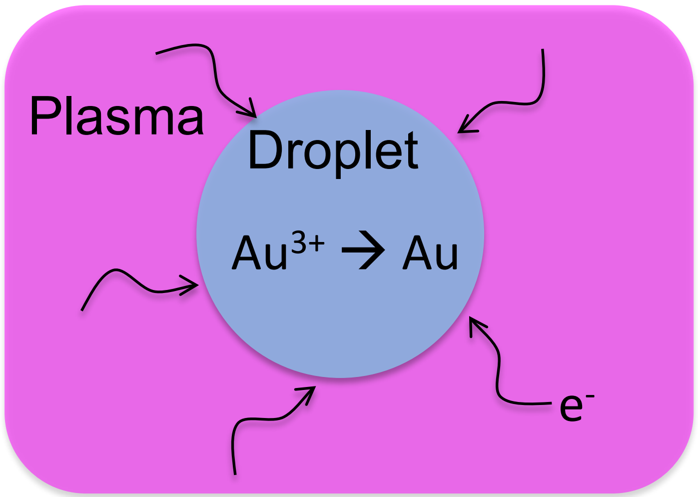

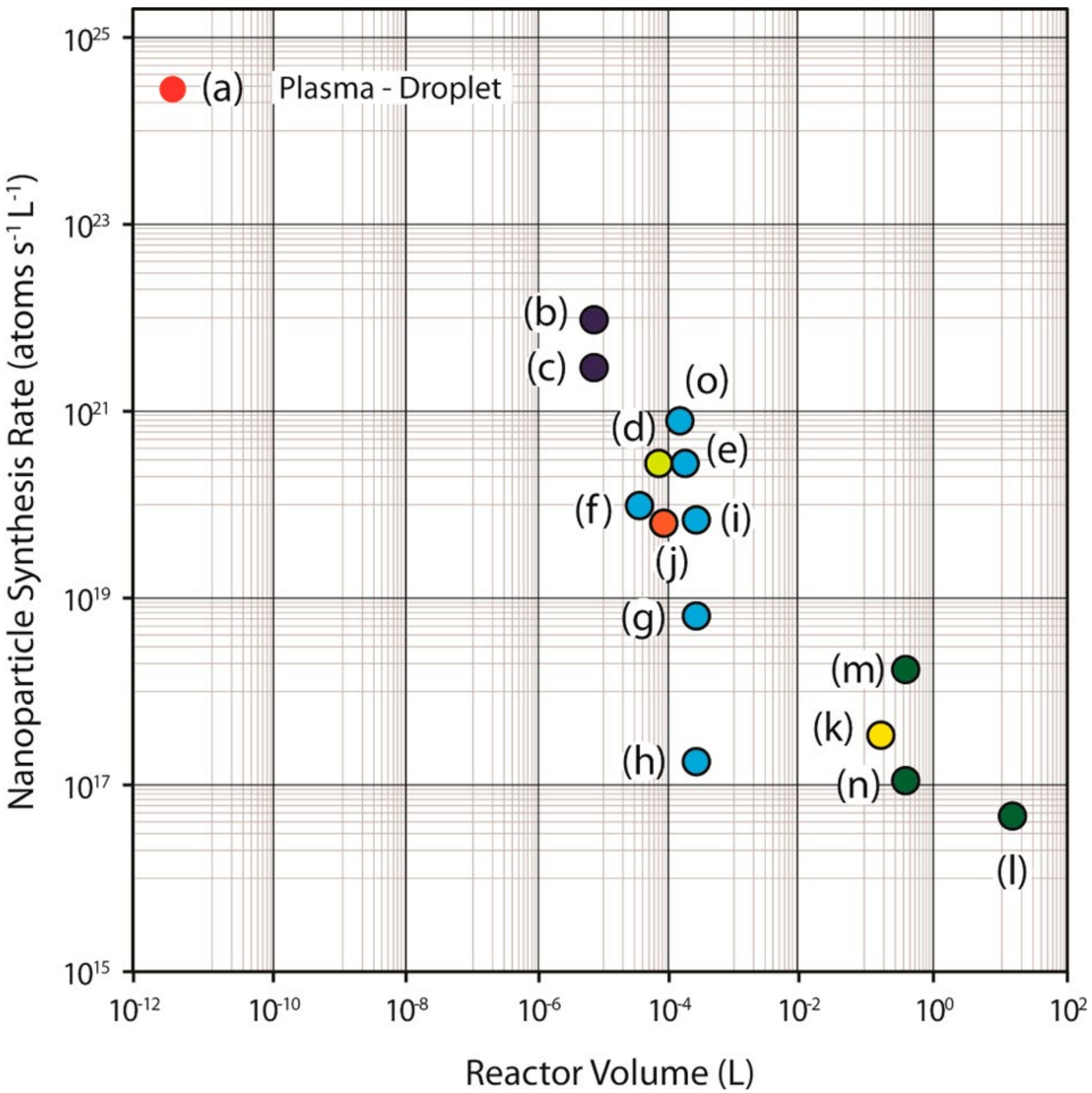

P. Maguire *et al.*, *Nano Lett.* **17**, 1336 (2017).

Plasma jet printing of metals from liquid aerosols

Space Foundry Inc., Moffett Field, CA

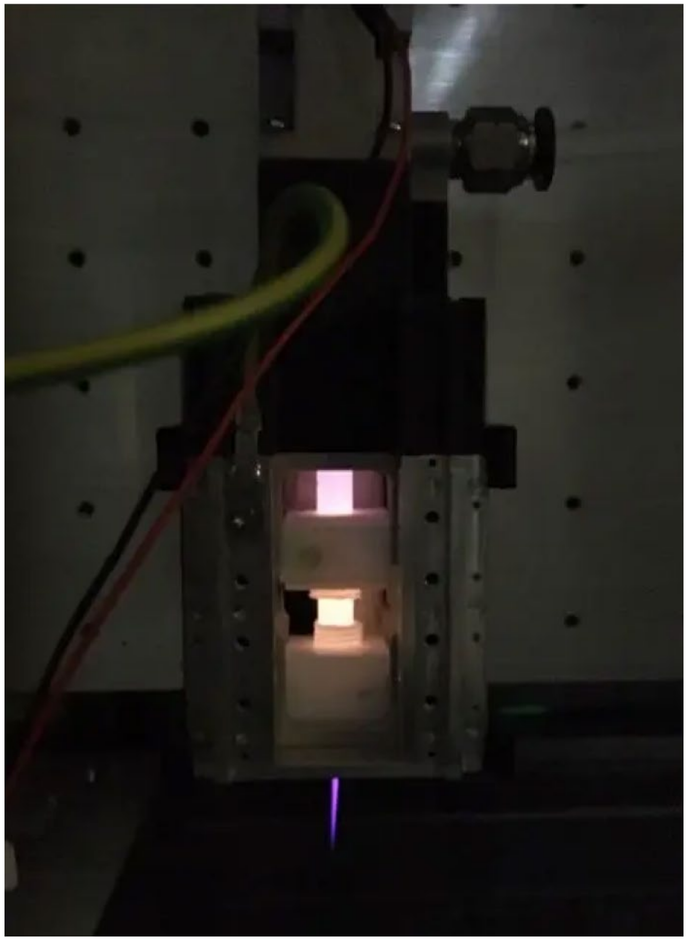

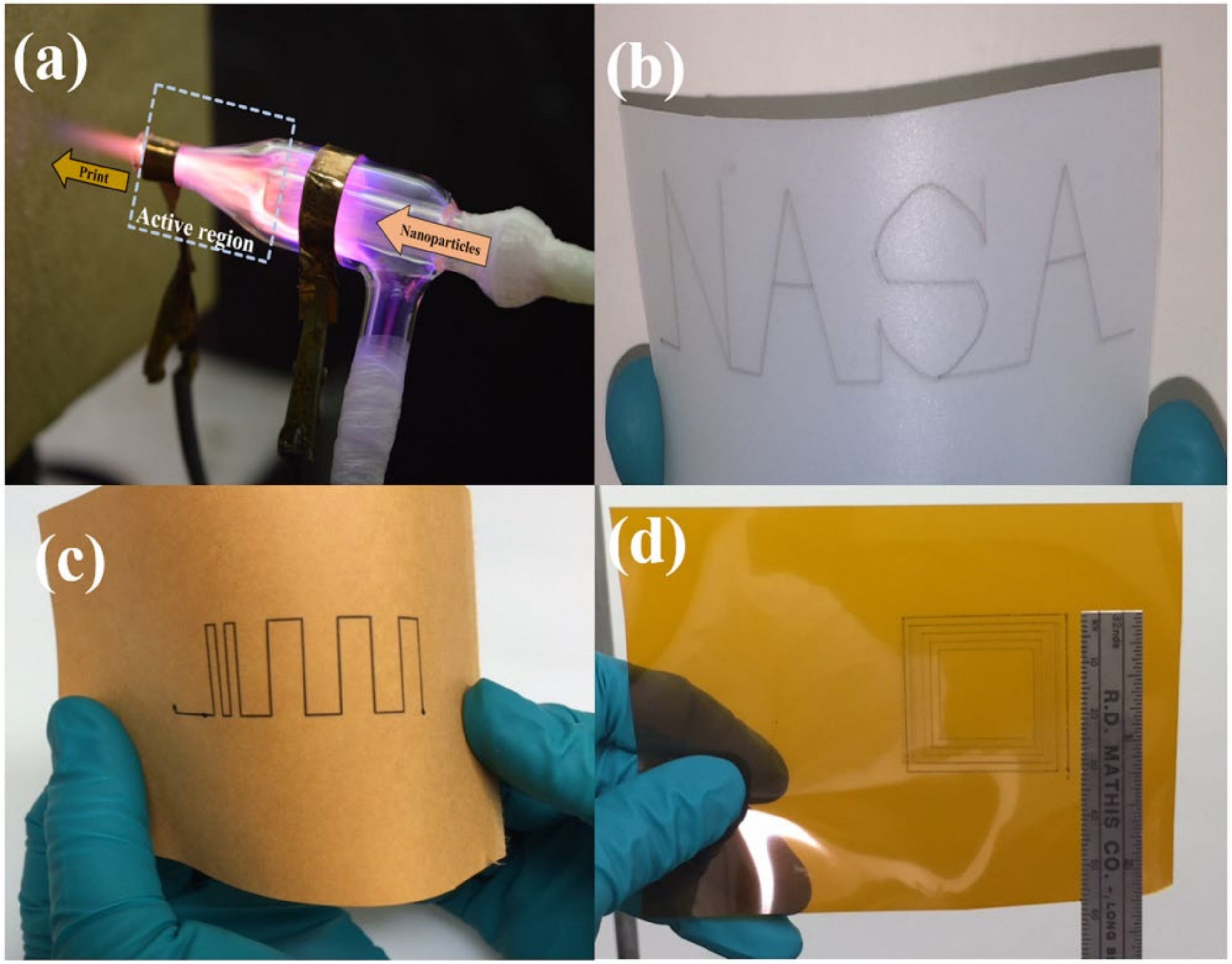

A. Dey *et al.*, *J. Vac. Sci. Technol. B* **37**, 031203 (2019).

I. Direct write
   a. Nanoparticle deposition
   b. Reduction of dispersed metal salts

II. Post-print
   a. Sintering
   b. Conversion
   c. Beyond metals

Localized conversion of thin films of metal precursor and polymer

Aqueous solution of polymer and metal salt

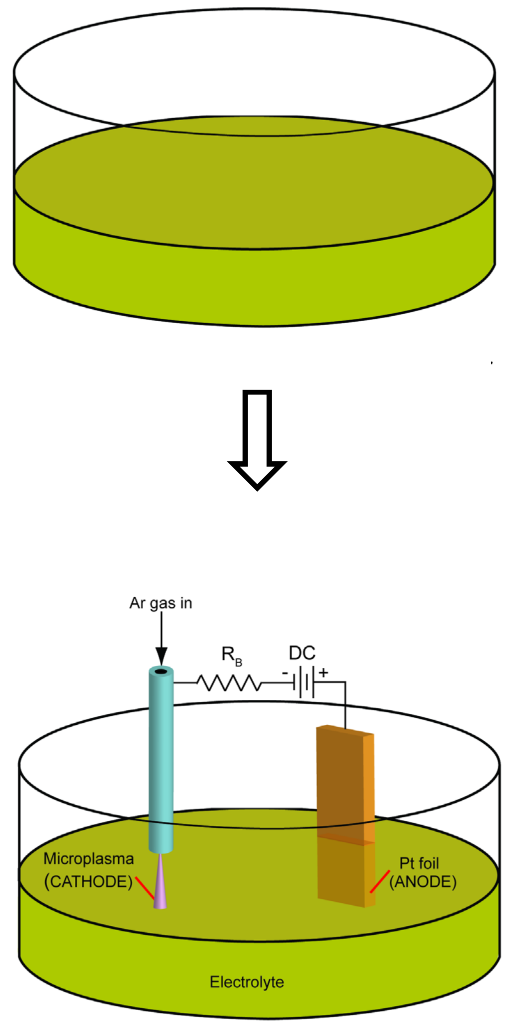

Localized conversion of thin films of metal precursor and polymer

Aqueous solution of polymer and metal salt

Doctor's blade coating (spin coating, etc.)

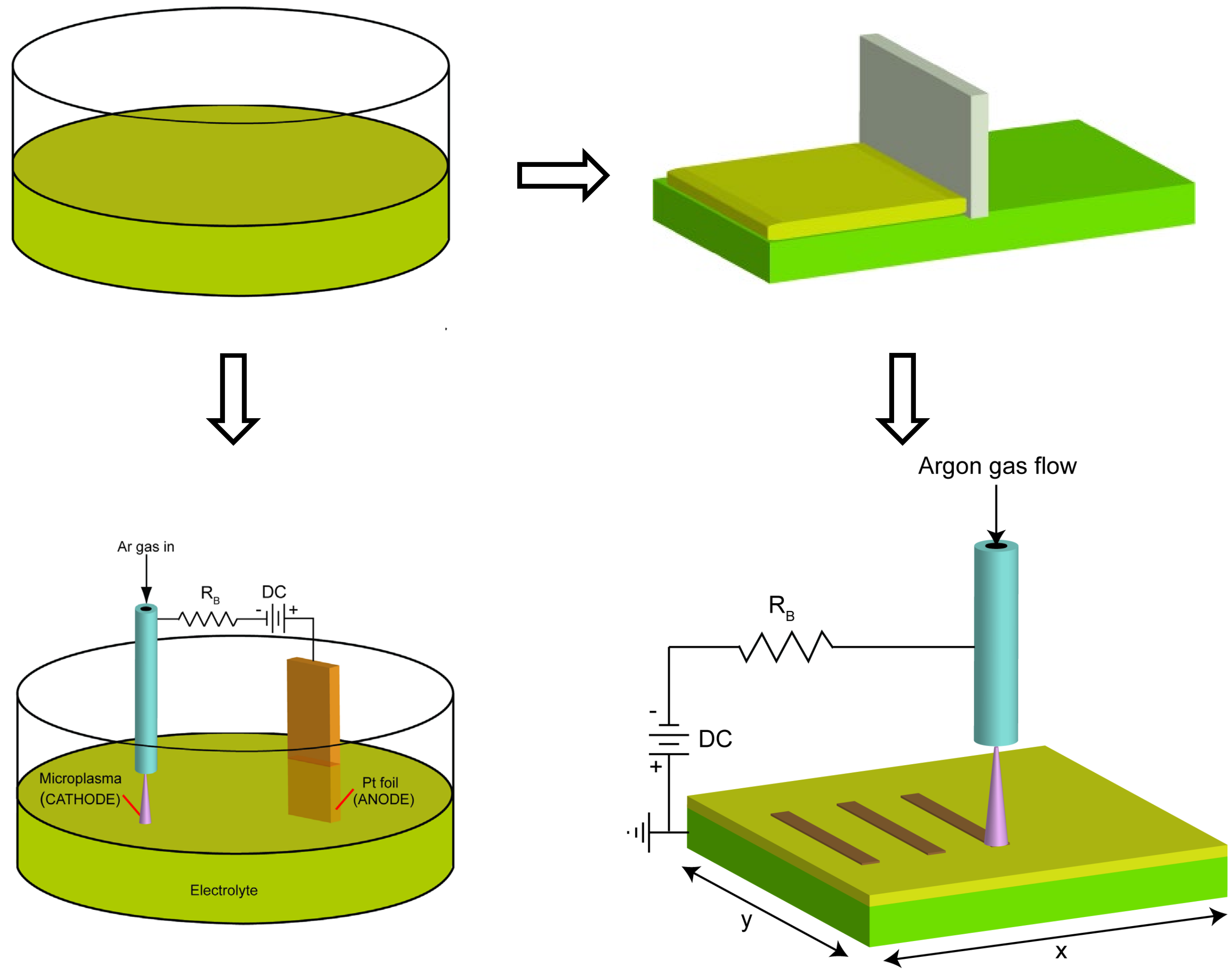

Electrical characterization of $AgNO_3$/PVA films

2-point probe measurement

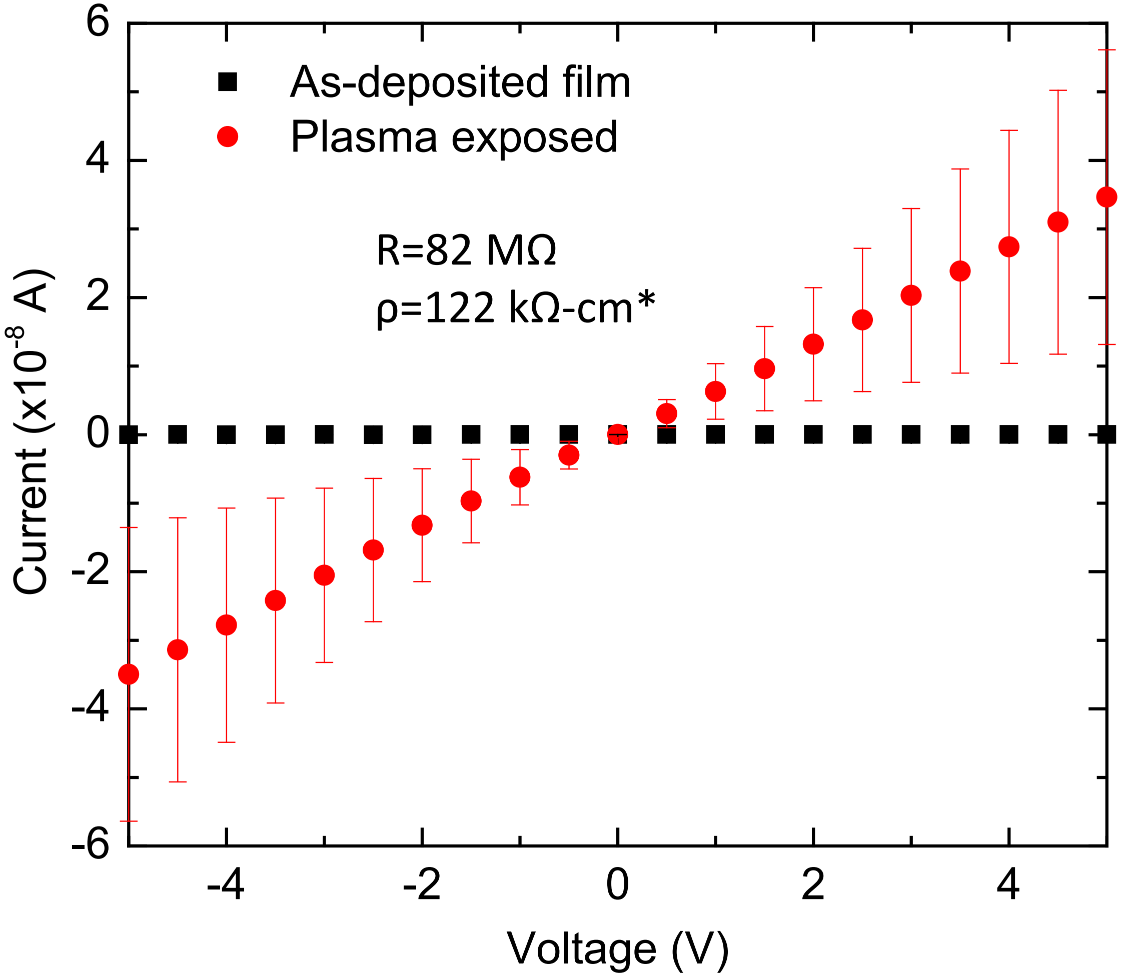

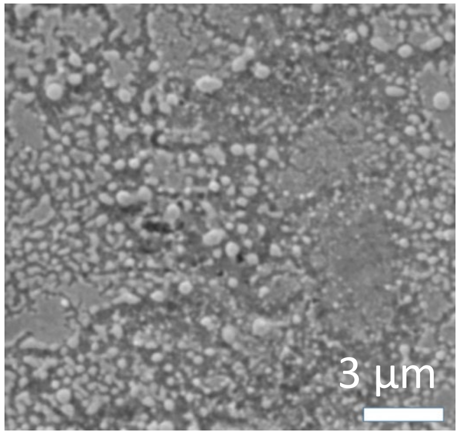

- Large resistance may be due to poor morphology (not completely percolating).
- At higher Ag precursor loading, solutions are unstable.

*Ag: 1.59 µΩ-cm

ACS Appl. Mater. Inter. **6**, 2099 (2014).

Polyacrylic acid as a polymer matrix

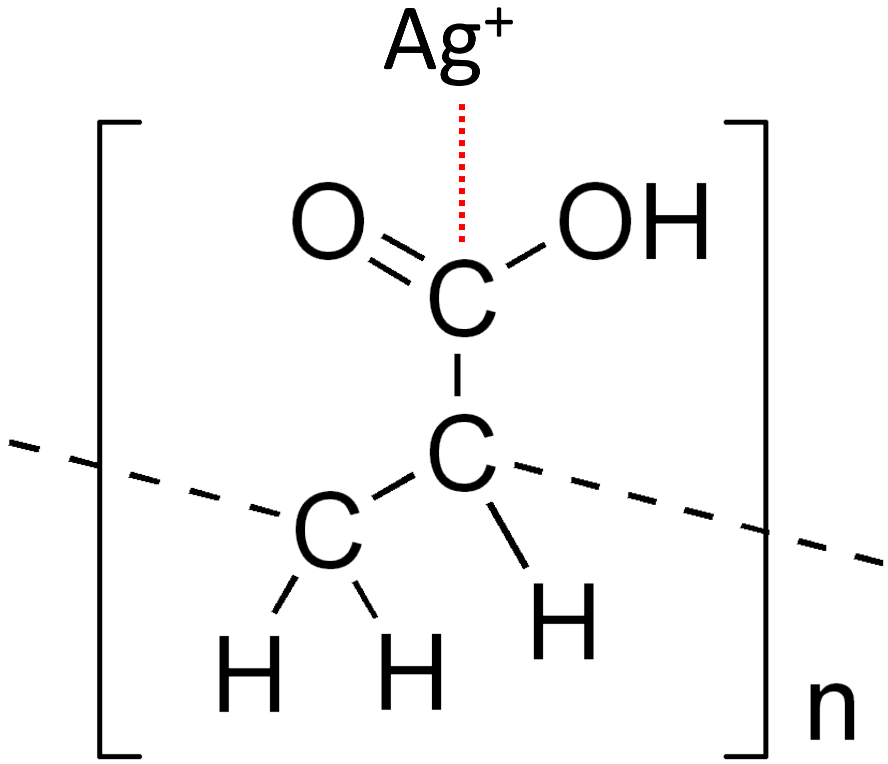

PAA$_r$:Ag$^+$ = 1:0.32

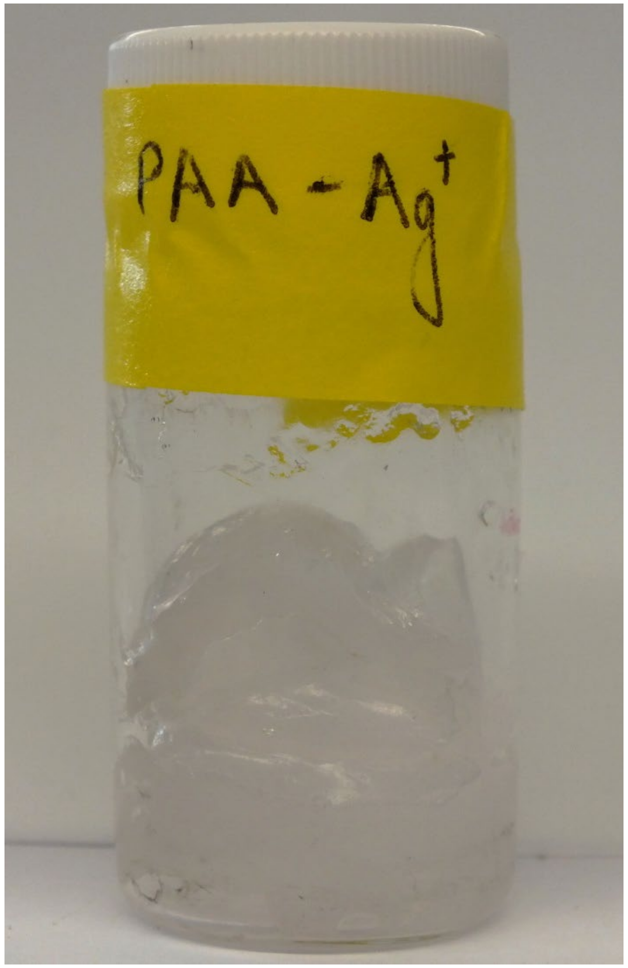

ACS Appl. Mater. Inter. **6**, 2099 (2014).

Polyacrylic acid as a polymer matrix

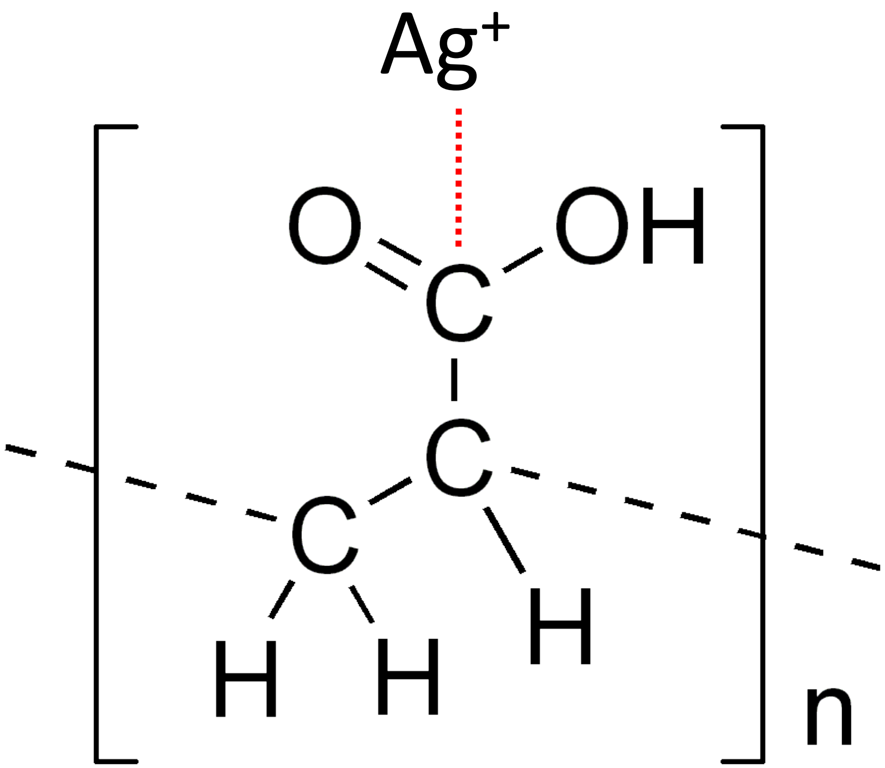

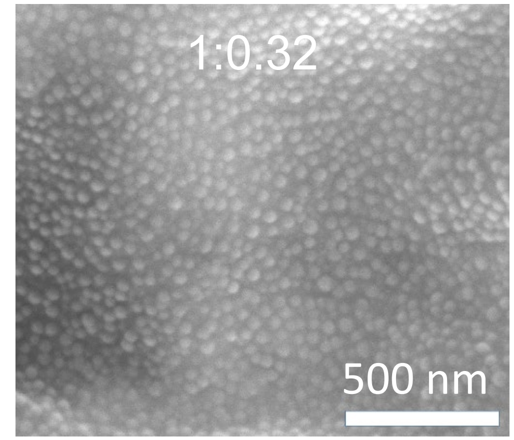

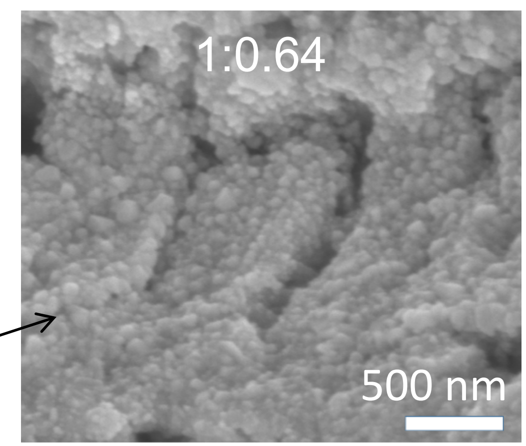

Percolating network

ACS Appl. Mater. Inter. **6**, 2099 (2014).

Cross-sectional EDS of microplasma-reduced Ag-PAA films

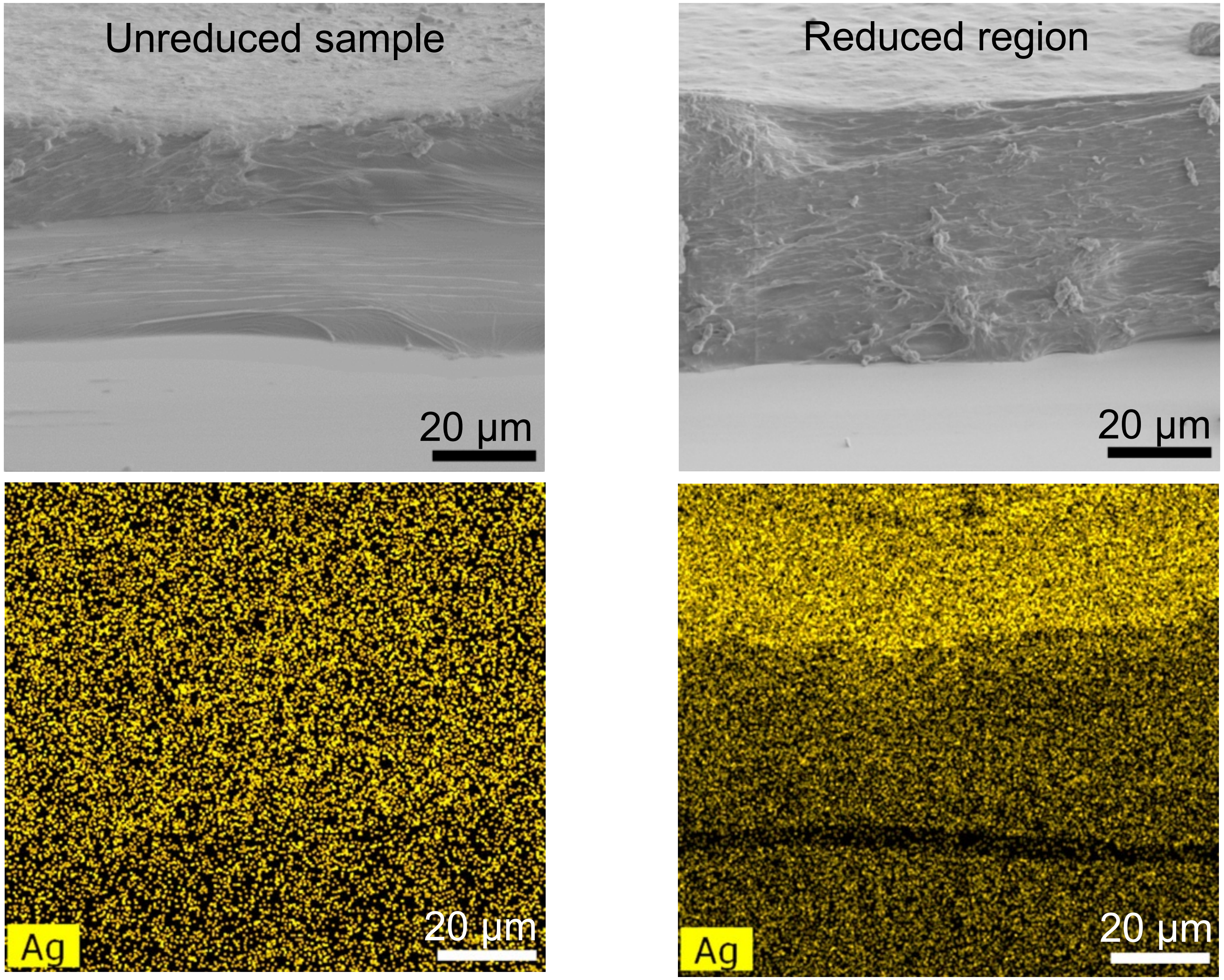

ACS Appl. Mater. Inter. **6**, 2099 (2014).

Proposed electric migration mechanism for surface-rich Ag layer

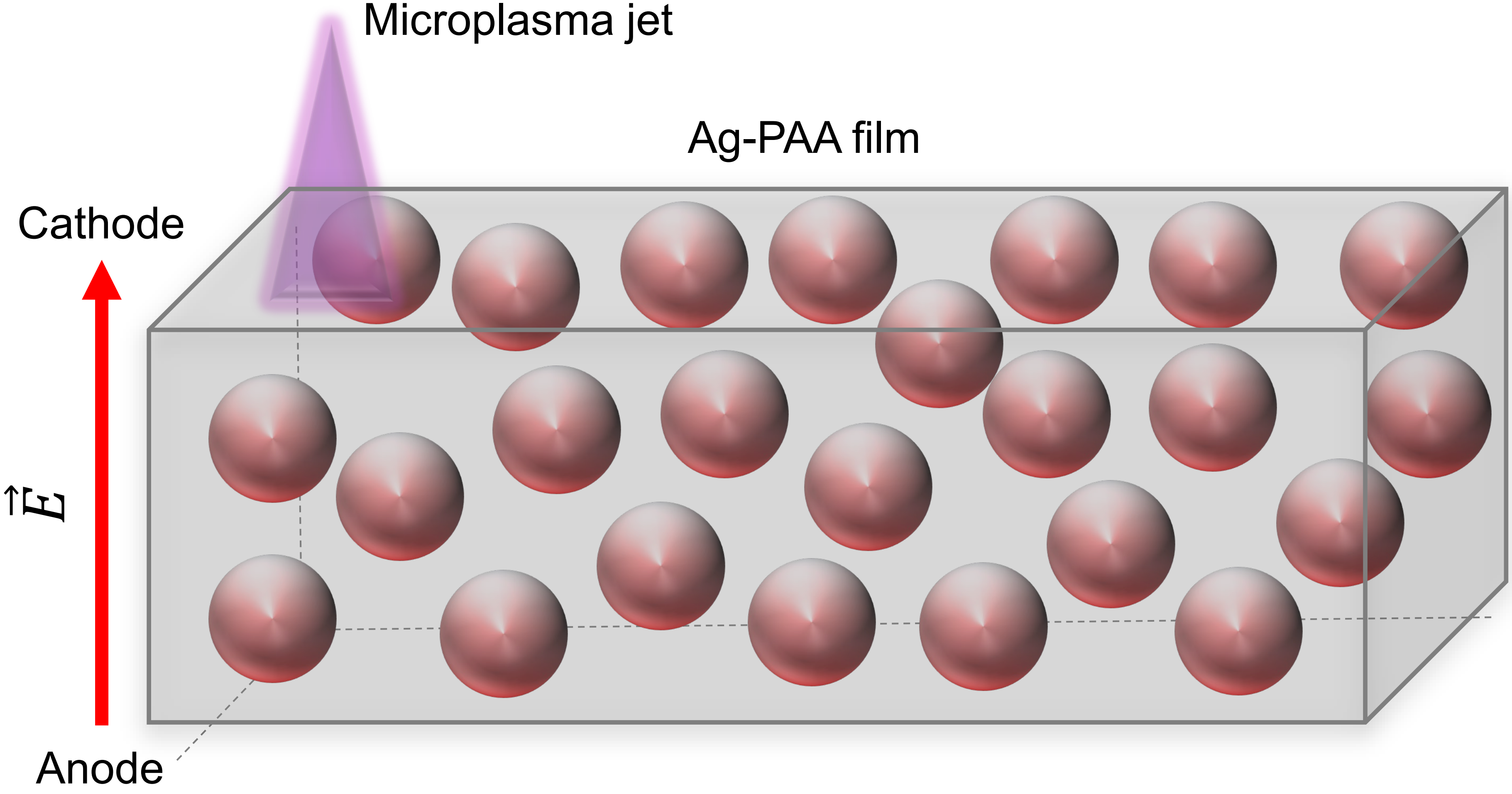

ACS Appl. Mater. Inter. **6**, 2099 (2014).
Plasma Chem. Plasma Proc. **36**, 295 (2016).

Electrical conductivity depends on initial film thickness

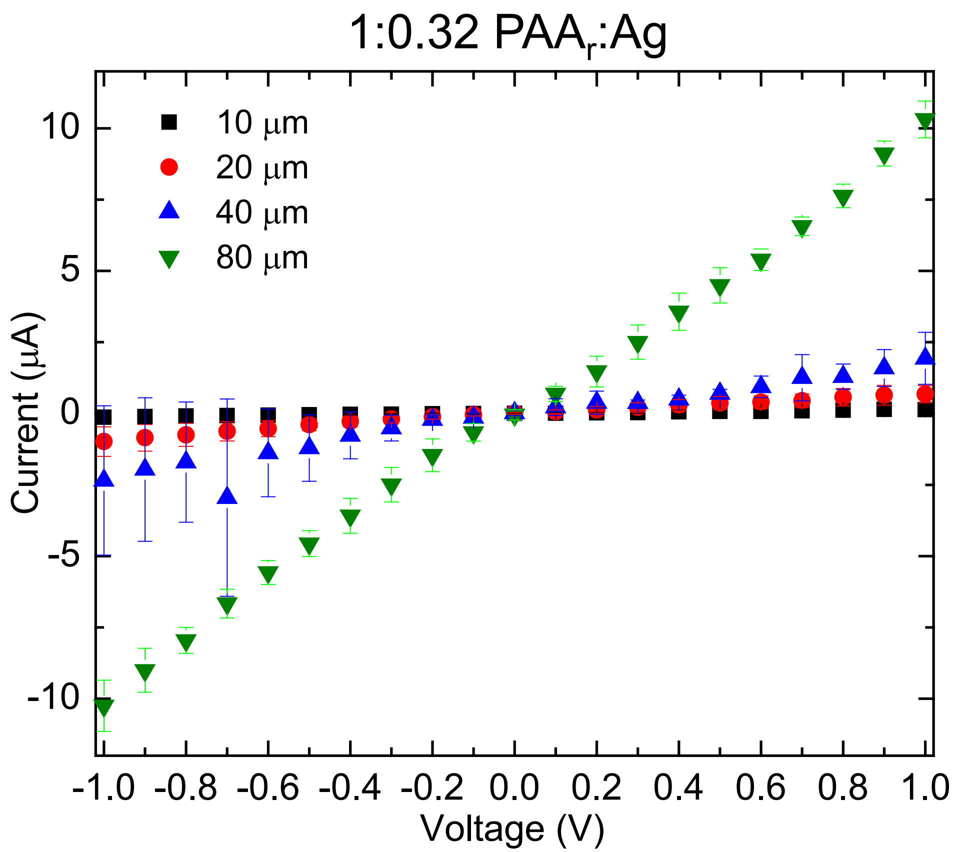

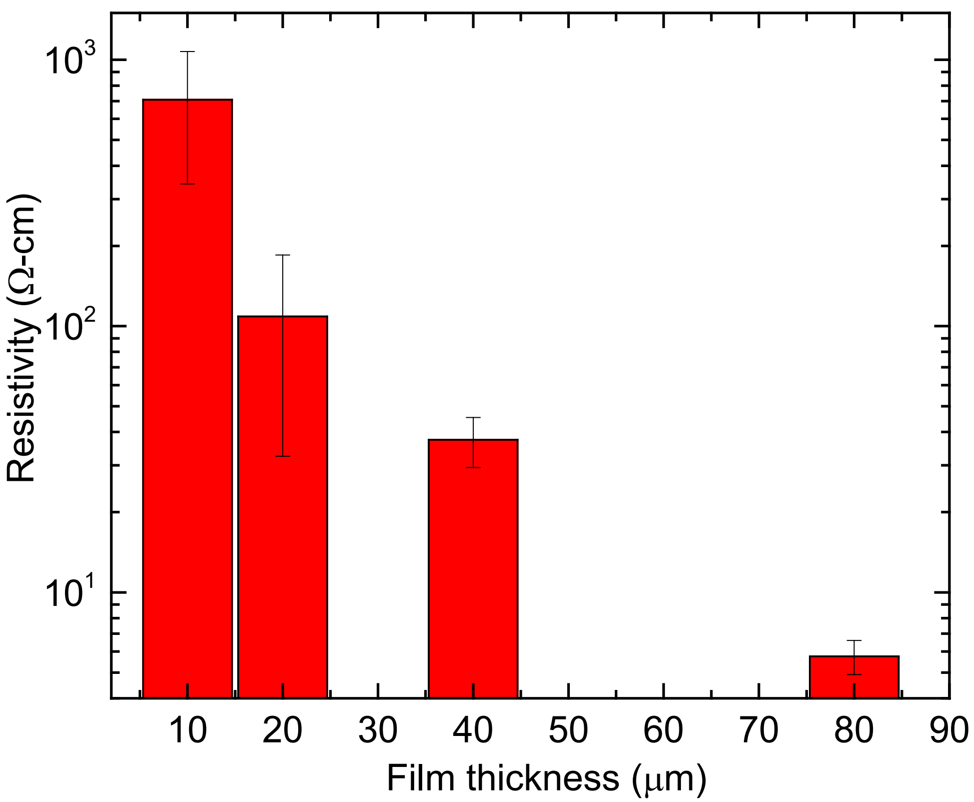

Film acts as a "reservoir" for the reduction and formation of Ag at the surface.

*Ag: 1.59 μΩ-cm
*ITO: 0.1 Ω-cm
*Ag NP inks: 5 μΩ-cm-10 Ω-cm

ACS Appl. Mater. Inter. **6**, 2099 (2014).

Integration of reduced Ag-PAA films with elastomeric PDMS substrates

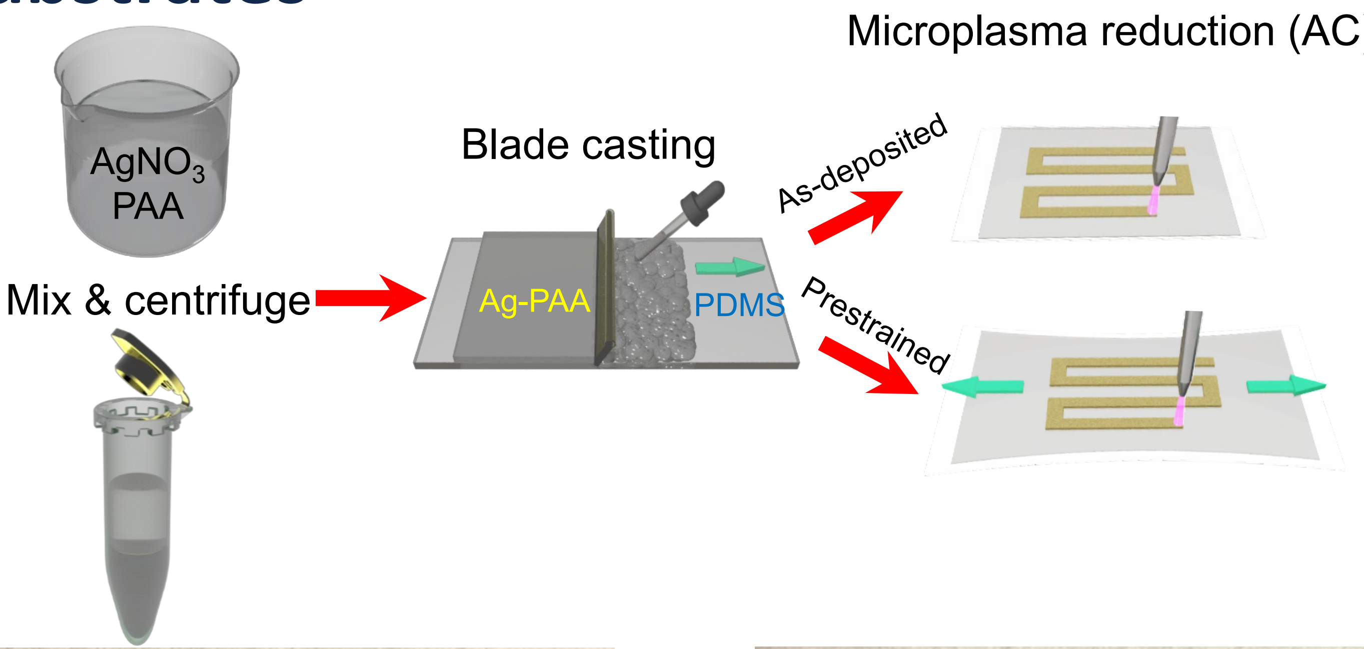

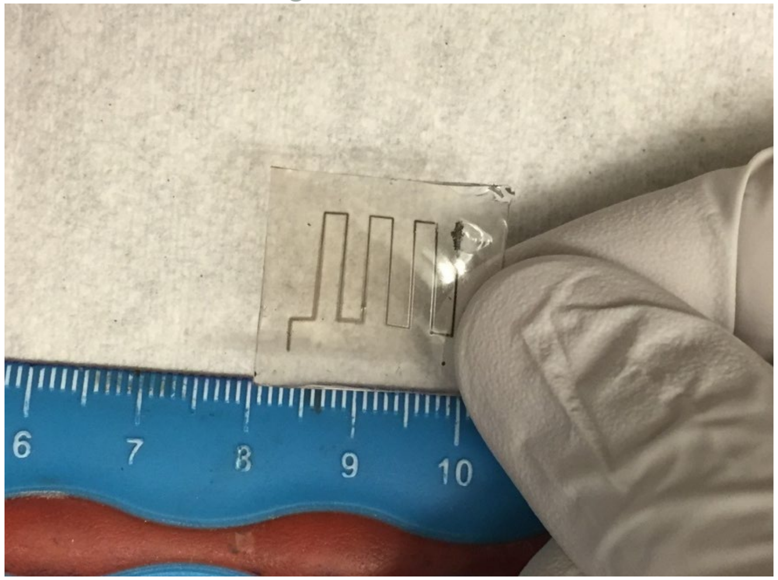

ACS Macro. Lett. **6**, 194 (2017).

Conductivity as a function of strain in Ag-PAA on PDMS films

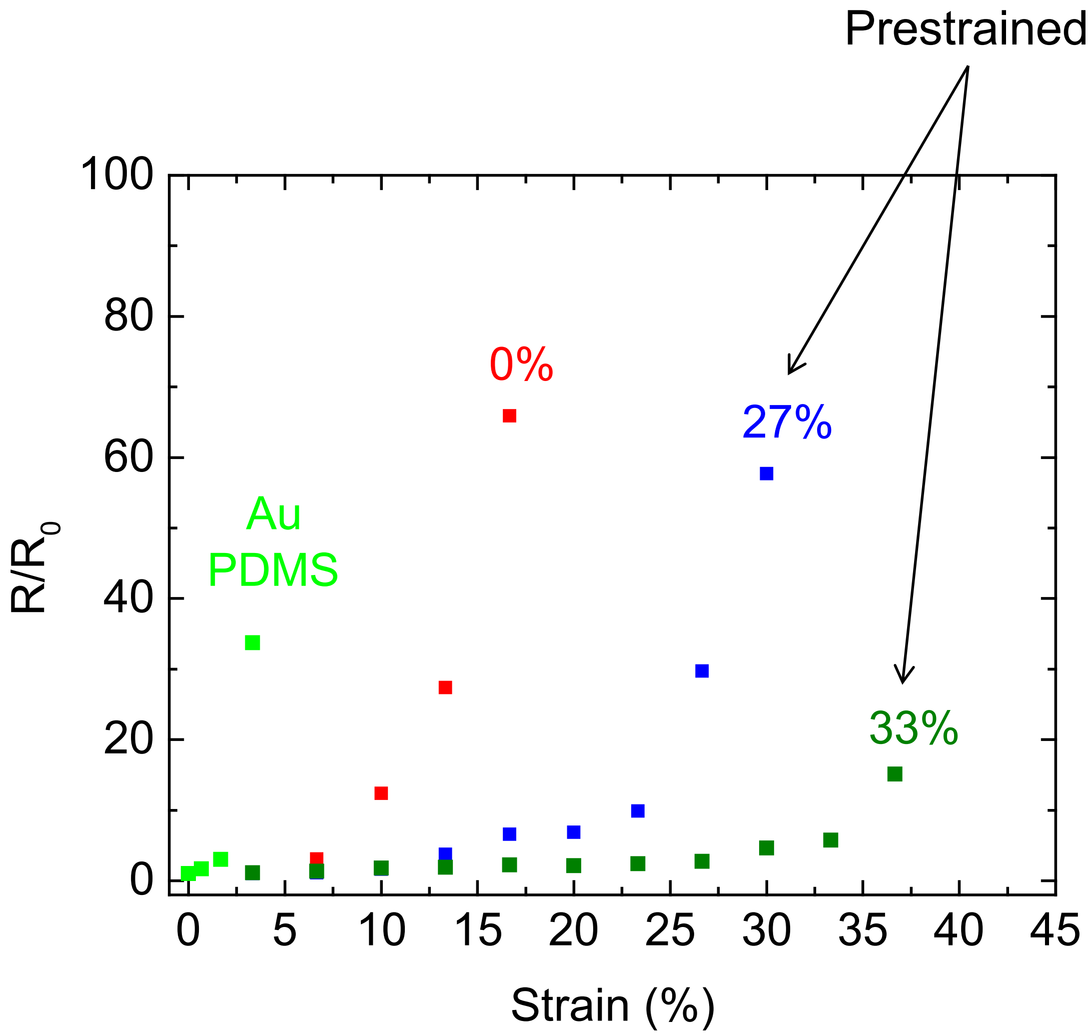

15%

27%

33%

ACS Macro. Lett. **6**, 194 (2017).

SEM analysis of microstructure during straining

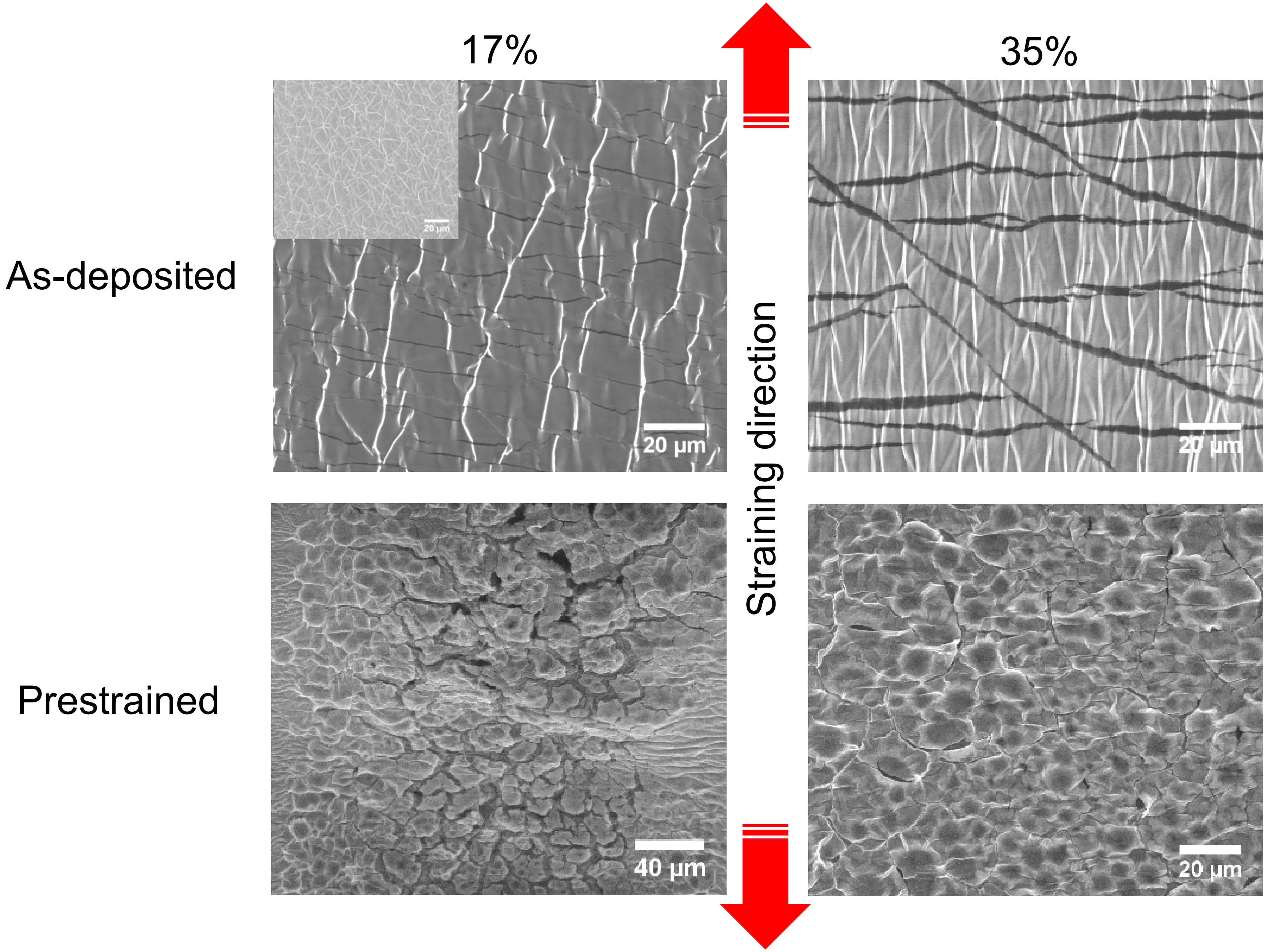

ACS Macro. Lett. **6**, 194 (2017).

I. Direct write
   a. Nanoparticle deposition
   b. Reduction of dispersed metal salts

II. Post-print
   a. Sintering
   b. Conversion
   c. Beyond metals

Need for sintering of printed nanoparticle inks

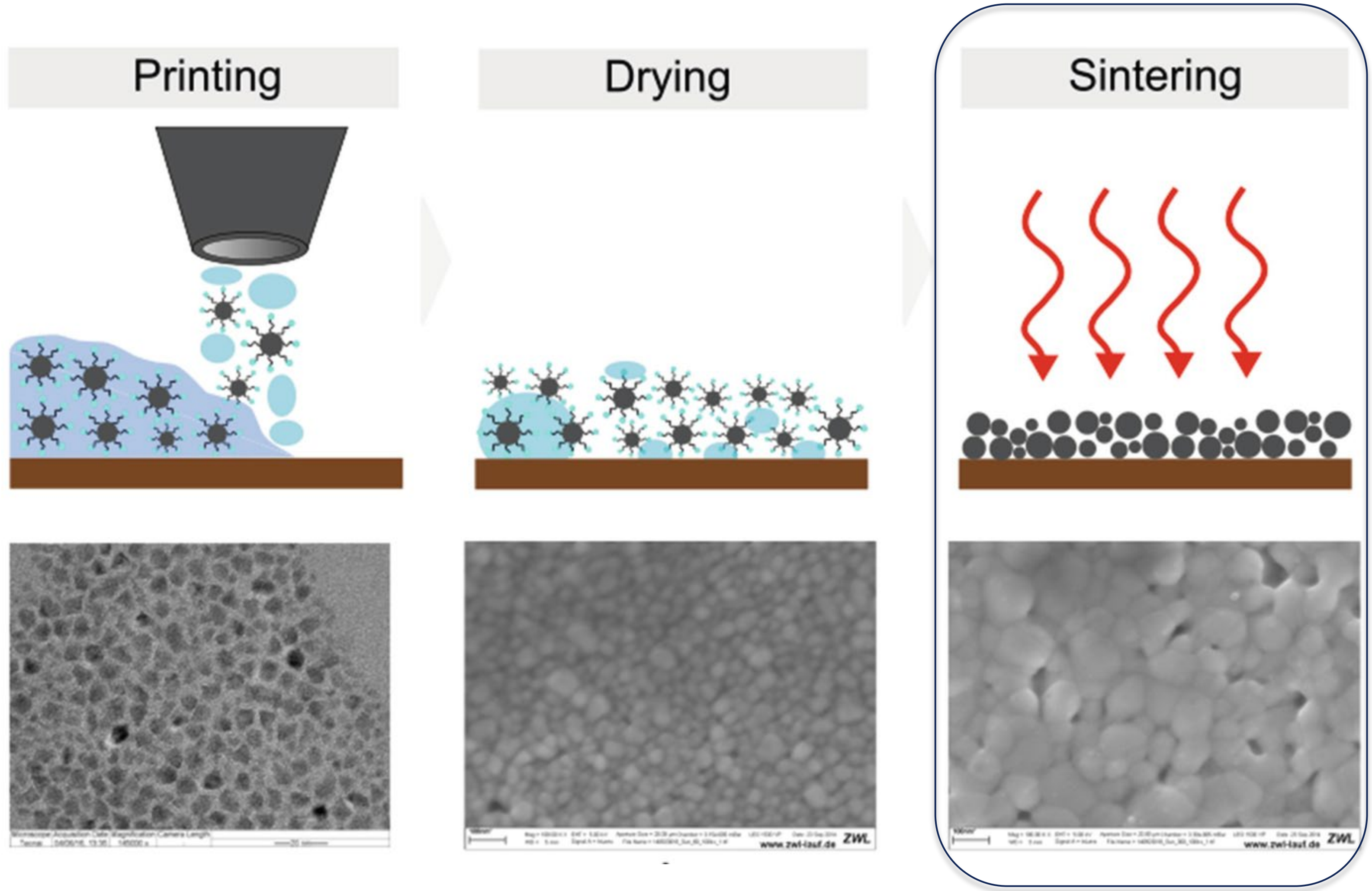

> 200 ^{o}C

< 150 ^{o}C

O. Kravchuk *et al.*, NANO 2017, 317 (2018).

Plasma sintering

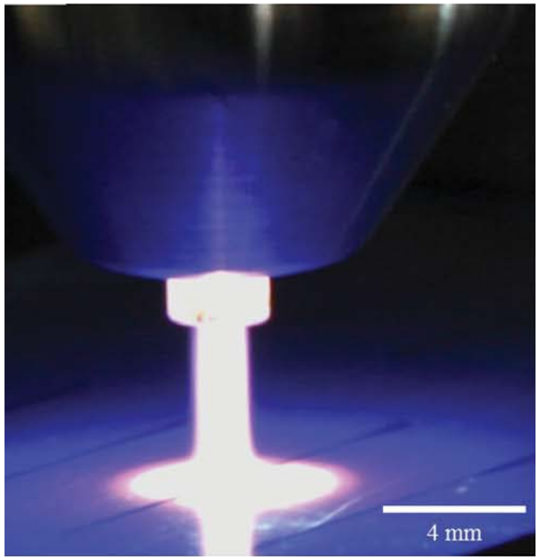

Table 1 Resistivity (ρ) of three inkjet printed silver NP inks after argon plasma sintering at atmospheric pressure and low pressure; resistivity values after thermal sintering according to data sheets (commercial inks) and experimental results (custom ink), respectively

	Cabot CCI-300	Harima NPS-J	Custom ink
	$\rho/\mu\Omega$ cm	$\rho/\mu\Omega$ cm	$\rho/\mu\Omega$ cm
Atm. p plasma (2 min)	16.1	25.4	13.0
Low p plasma (2 min)	3.6×10^4	5.0×10^5	207
Low p plasma (60 min)	91.5	13.4	15.2
Thermal (2 min)	18.8[a]	Not conductive[b]	Not conductive[a]
Thermal (60 min)	14.0[a]	3.0[b]	4.6[a]

[a] A sintering temperature of 150 °C was used. [b] A sintering temperature of 230 °C was used.

S. Wunscher *et al.*, *J. Mater. Chem.* **22**, 24569 (2012).

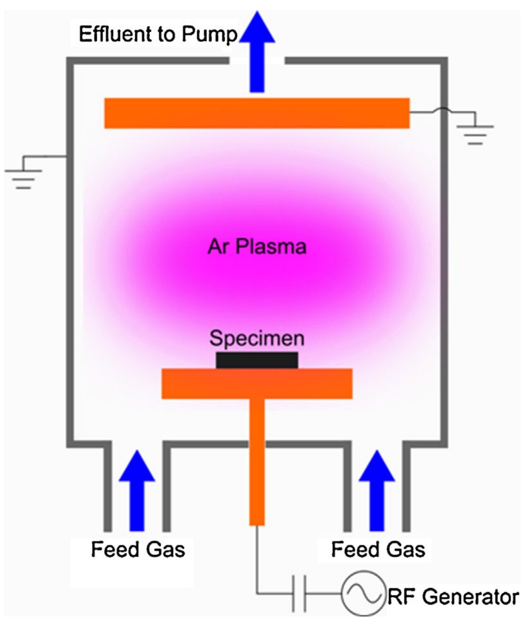

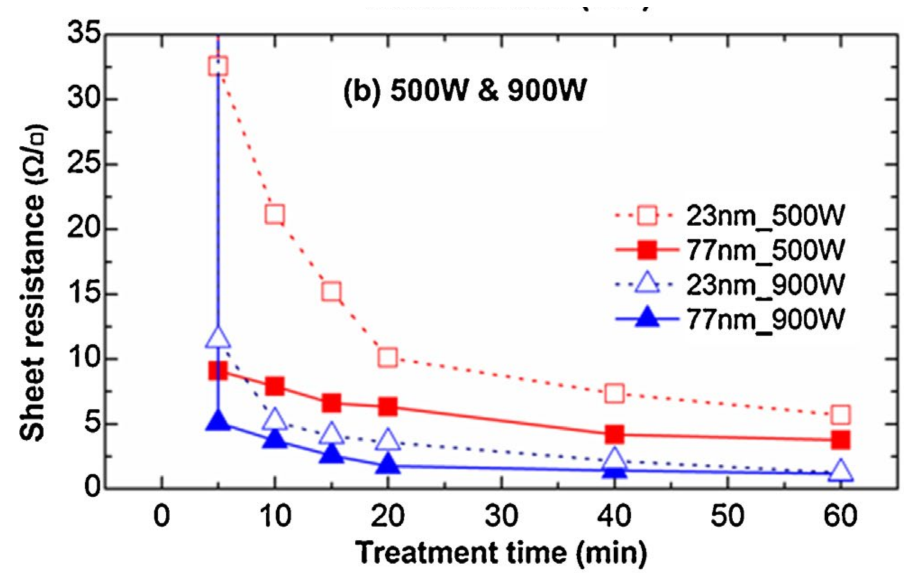

S. Ma *et al.*, *Appl. Surf. Sci.* **293**, 207 (2014).

I. Direct write
    a. Nanoparticle deposition
    b. Reduction of dispersed metal salts

II. Post-print
    a. Sintering
    b. Conversion
    c. Beyond metals

Plasma conversion: Metal-organic decomposition (MOD) inks

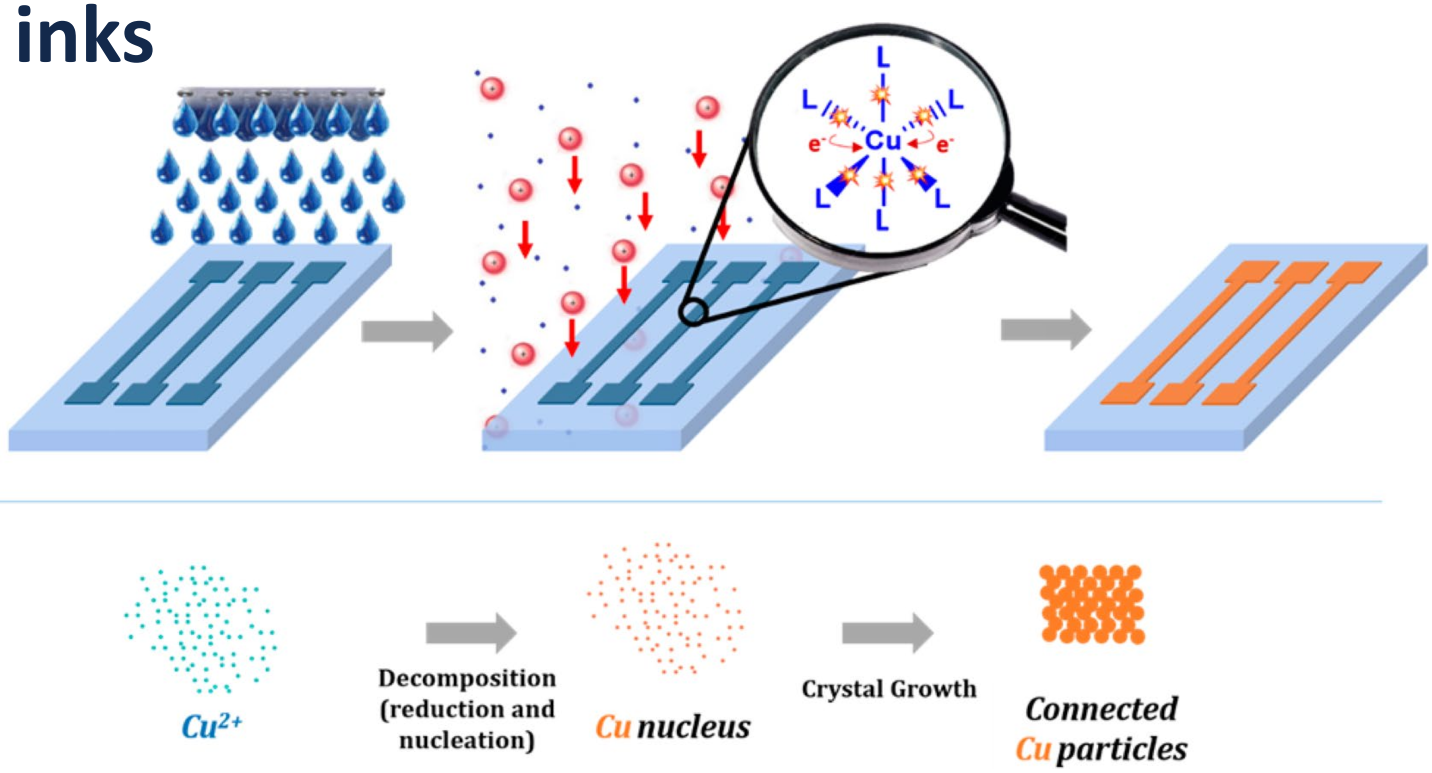

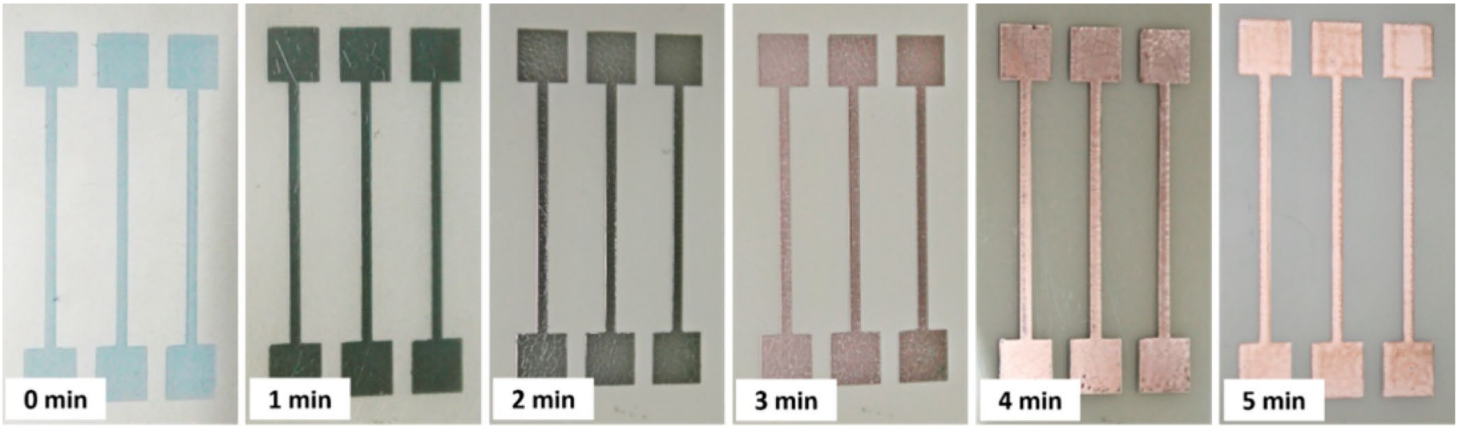

< 60 ^{o}C

Y. Farraj *et al.*, *ACS Appl. Mater. Inter.* **9**, 8766 (2017).

Plasma conversion: Metal-organic decomposition (MOD) inks

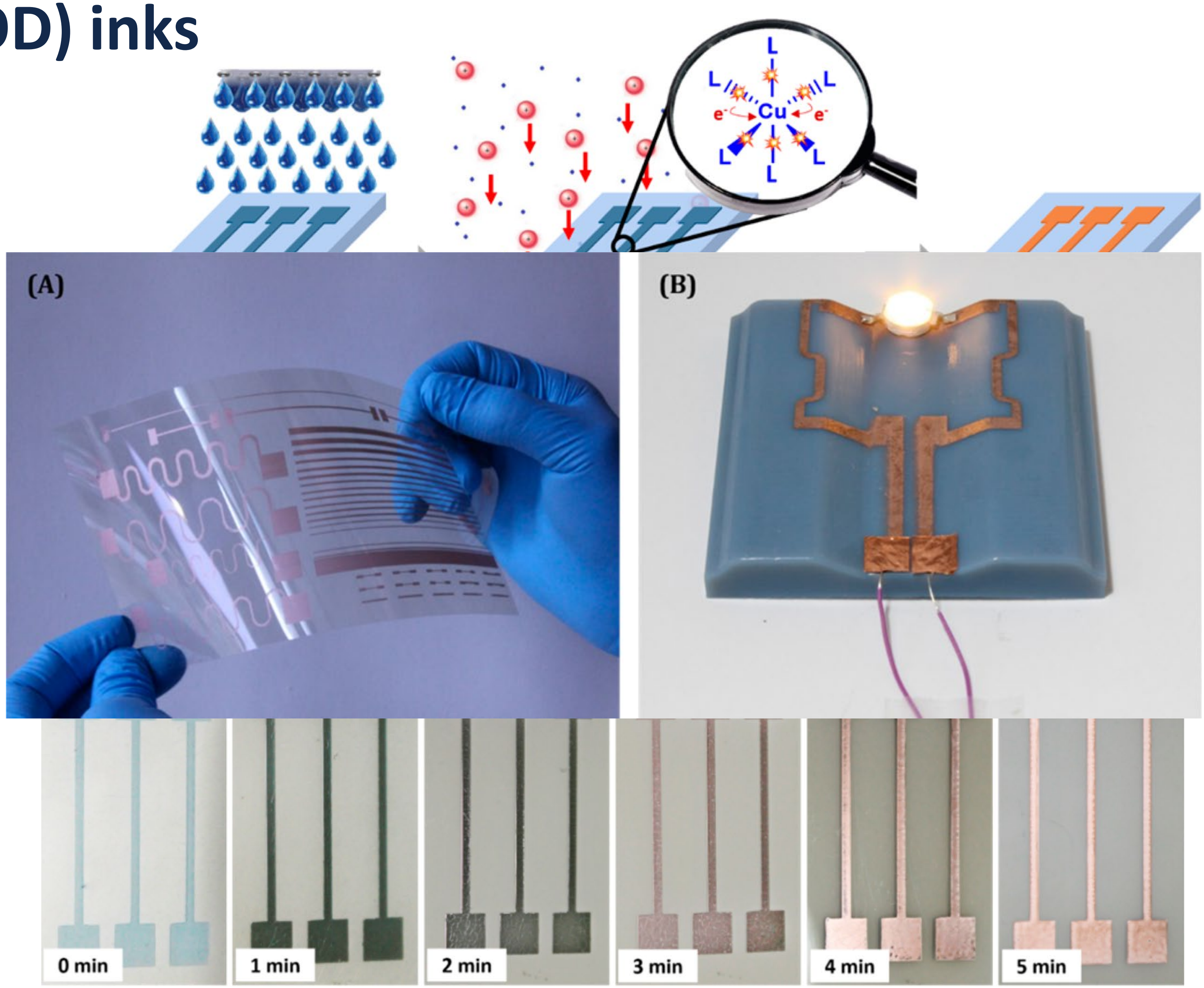

< 60 ^{o}C

Y. Farraj *et al.*, *ACS Appl. Mater. Inter.* **9**, 8766 (2017).

Plasma conversion: Metal salts dispersed in aqueous solutions

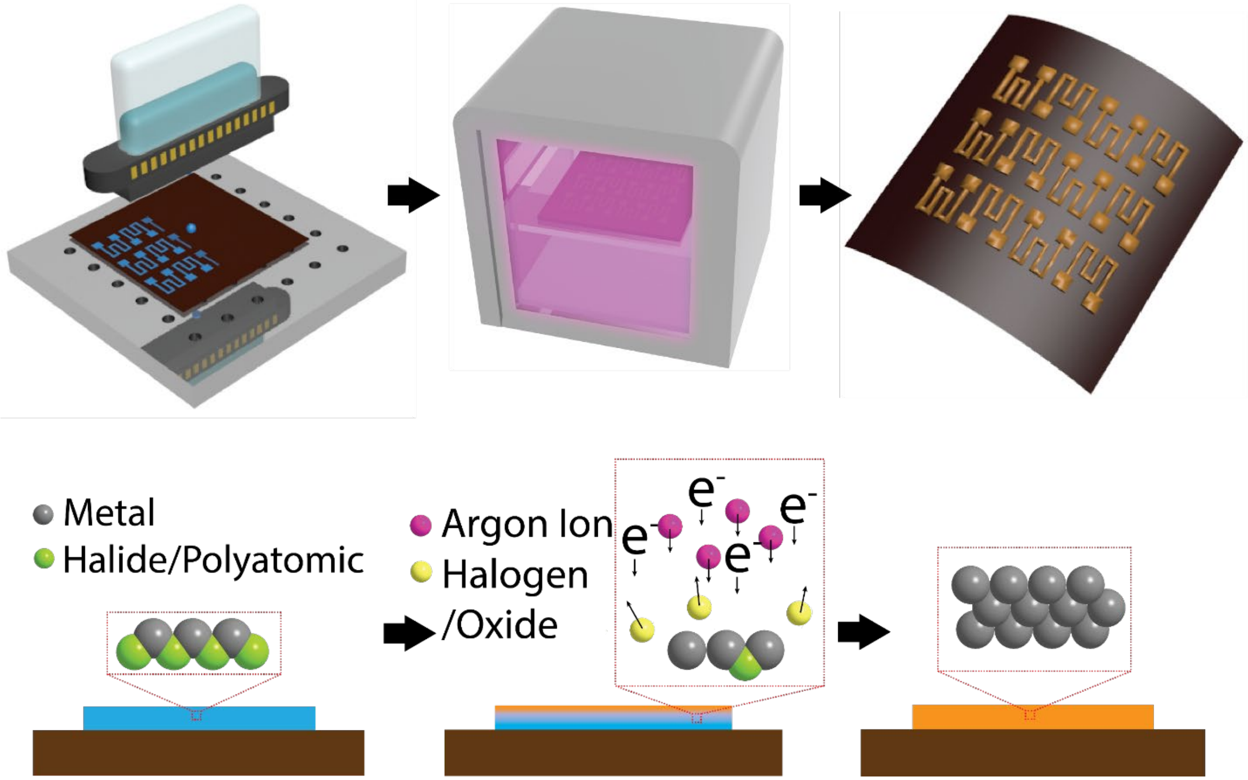

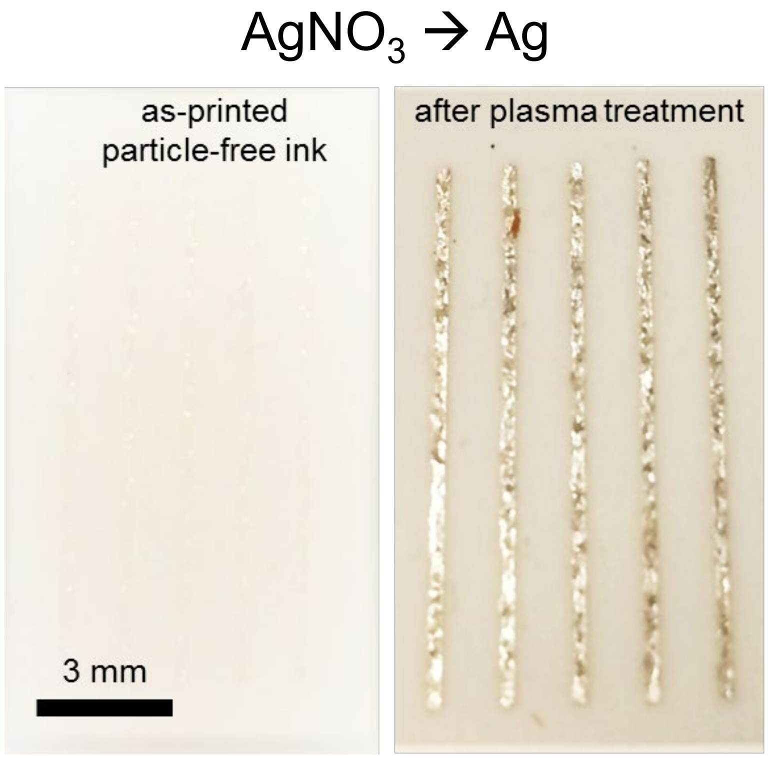

J. Vac. Sci. Technol. A **36**, 051302 (2018).

Plasma conversion: Metal salts dispersed in aqueous solutions

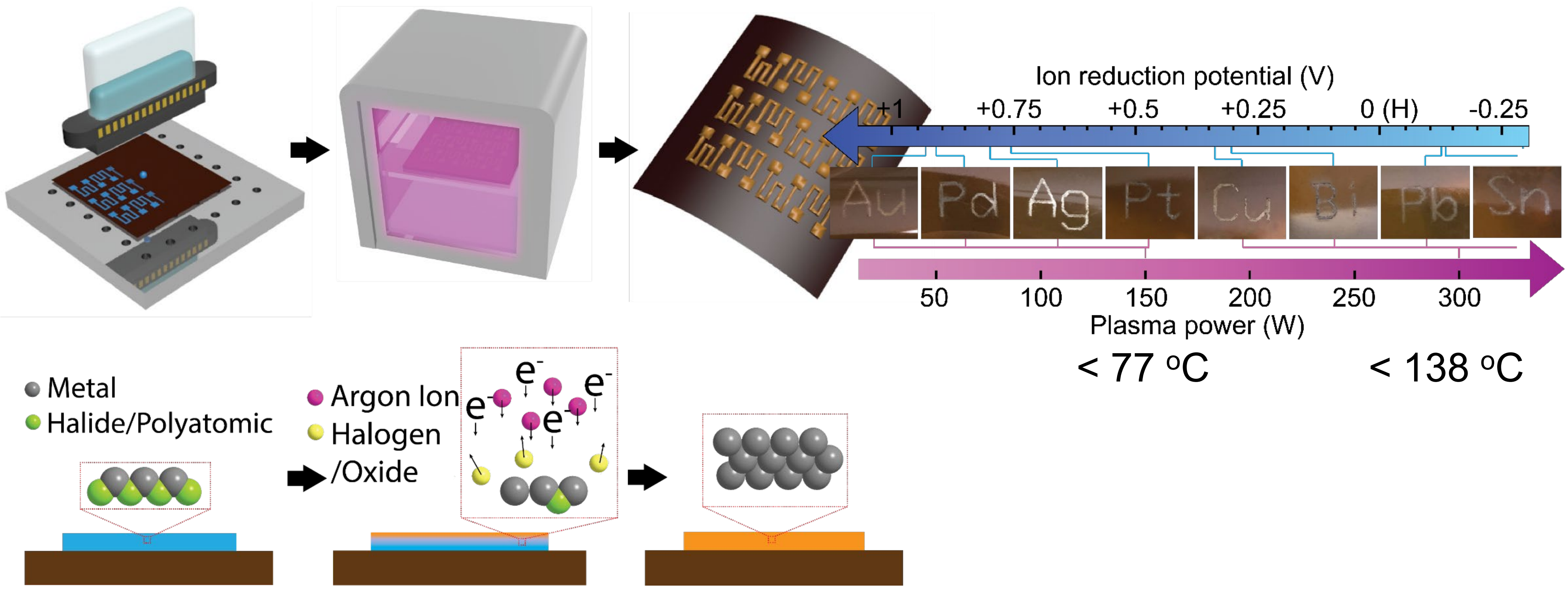

Adv. Mater. Technol. **4**, 1900119 (2019).

Plasma conversion: Metal salts dispersed in aqueous solutions

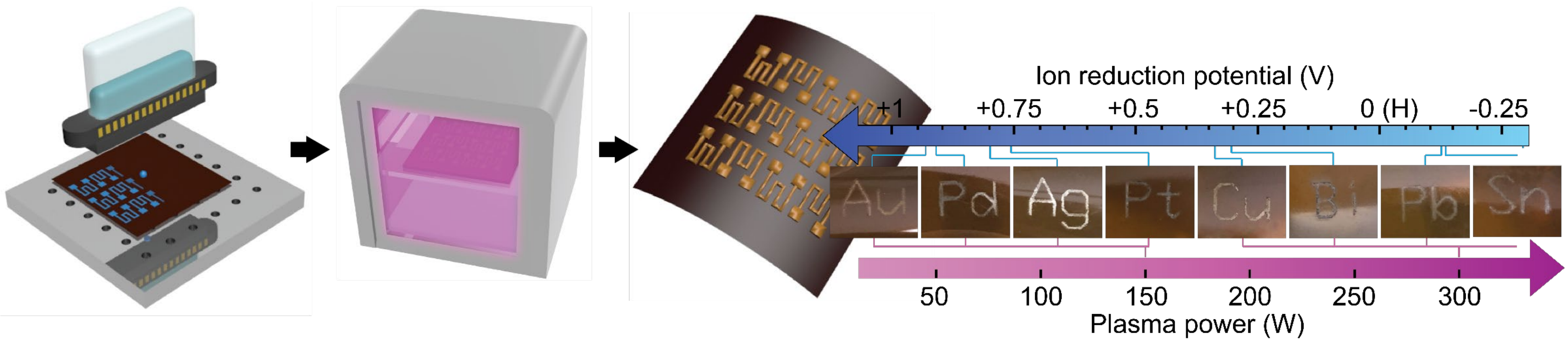

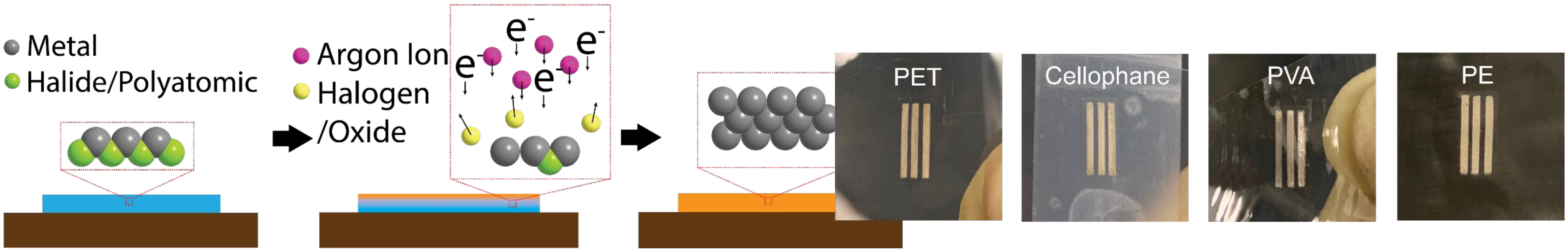

T_g ~ 75 ^oC 80 ^oC 100 ^oC (melting)

Characterization of printed and plasma converted metals

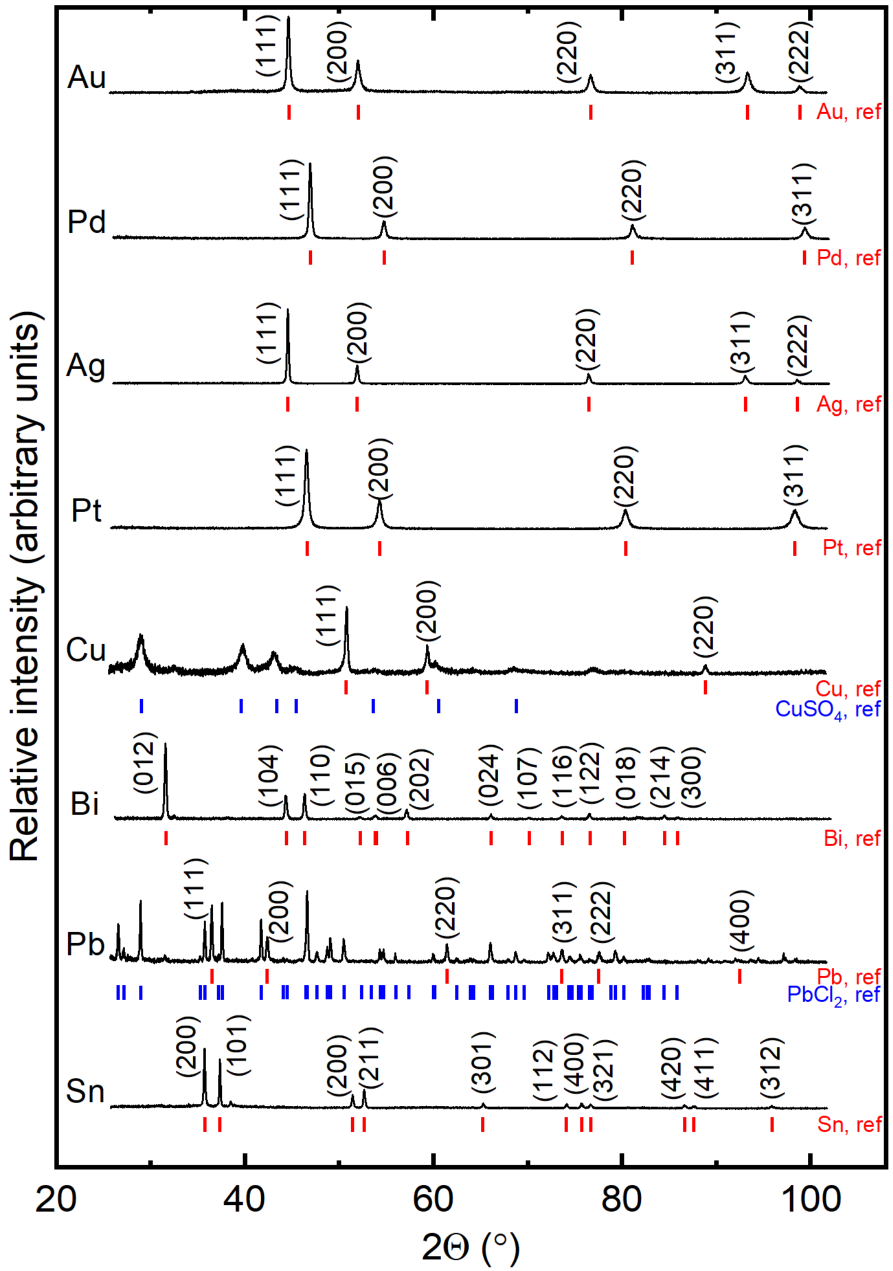

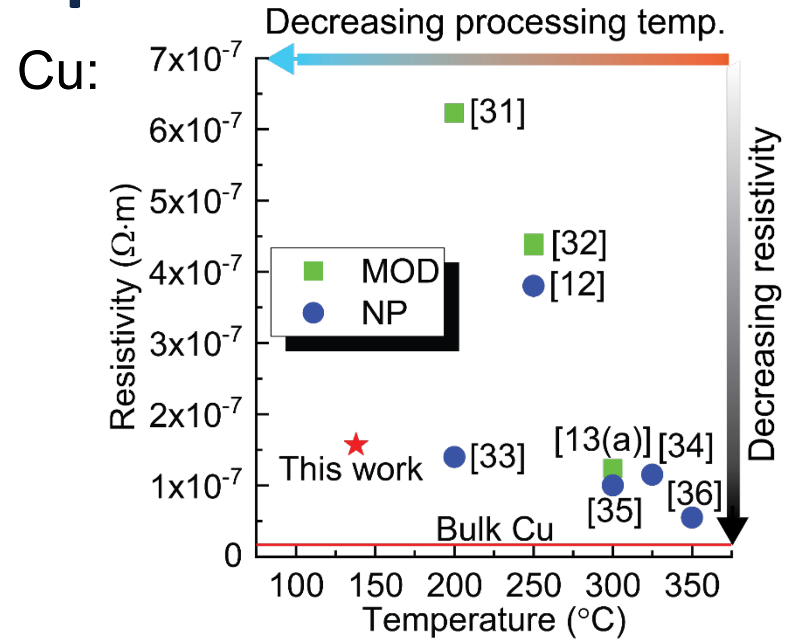

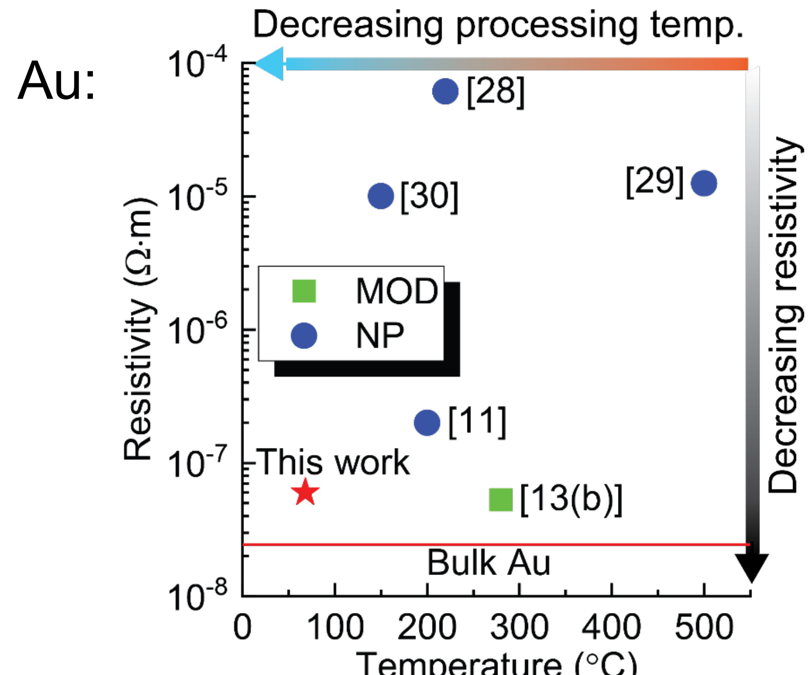

Adv. Mater. Technol. **4**, 1900119 (2019).

Potential mechanism for plasma conversion of printed metal salt films

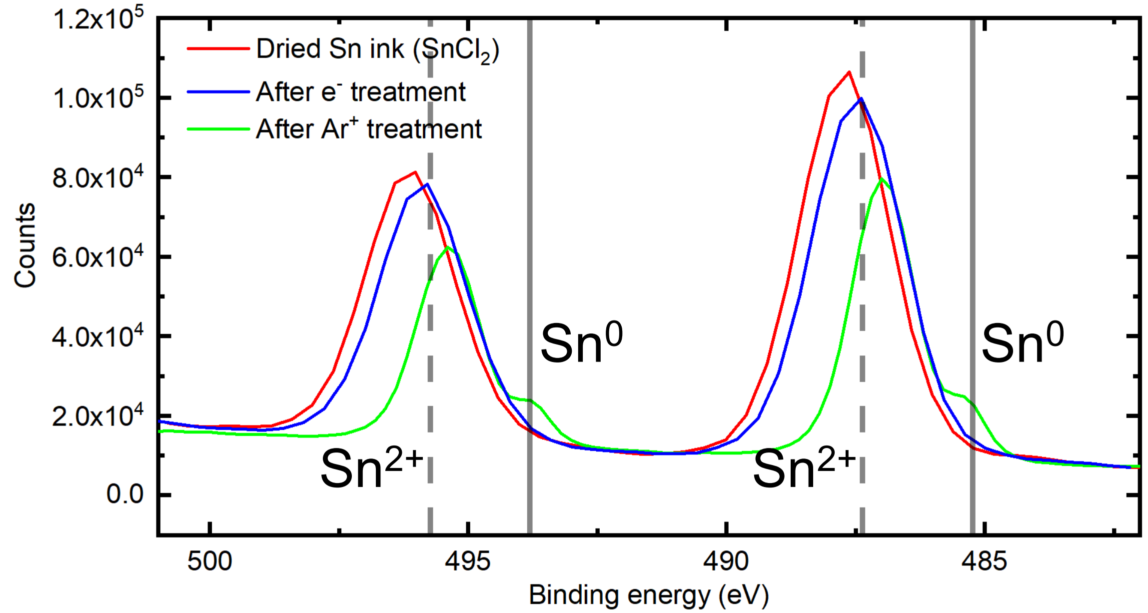

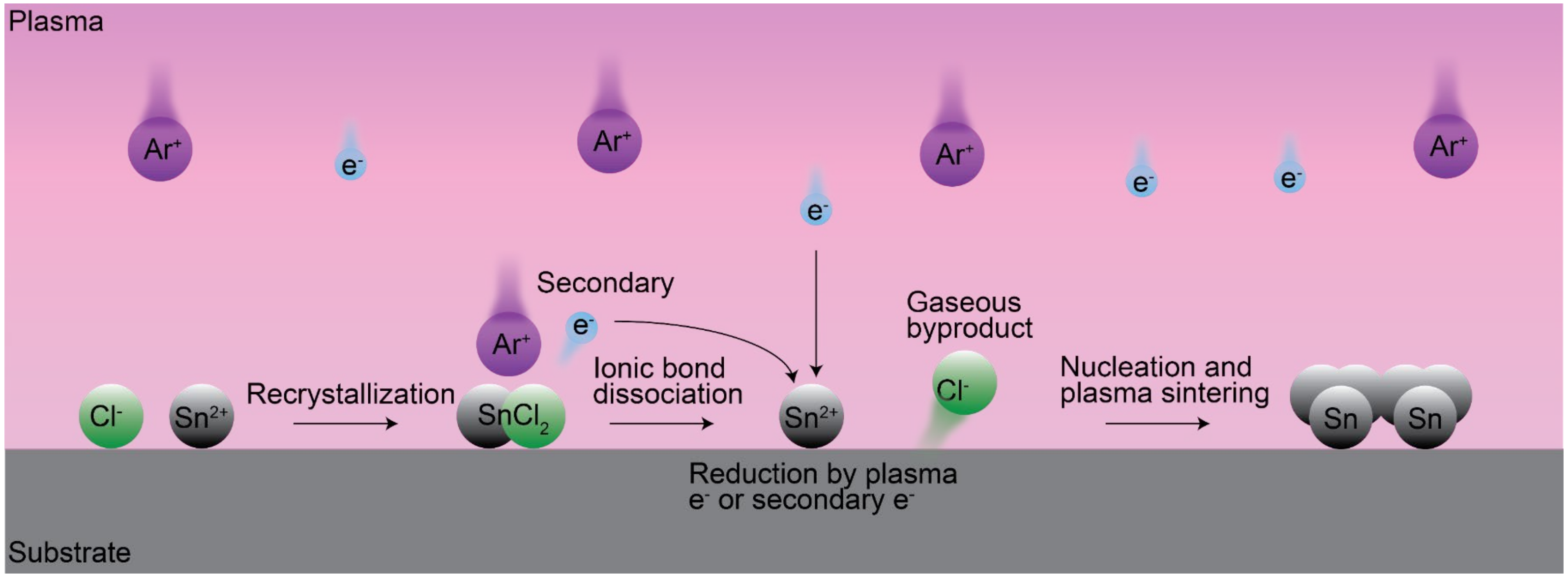

Adv. Mater. Technol. **4**, 1900119 (2019).

I. Direct write
   a. Nanoparticle deposition
   b. Reduction of dispersed metal salts

II. Post-print
   a. Sintering
   b. Conversion
   c. Beyond metals

Plasma conversion (reduction) of graphene oxide

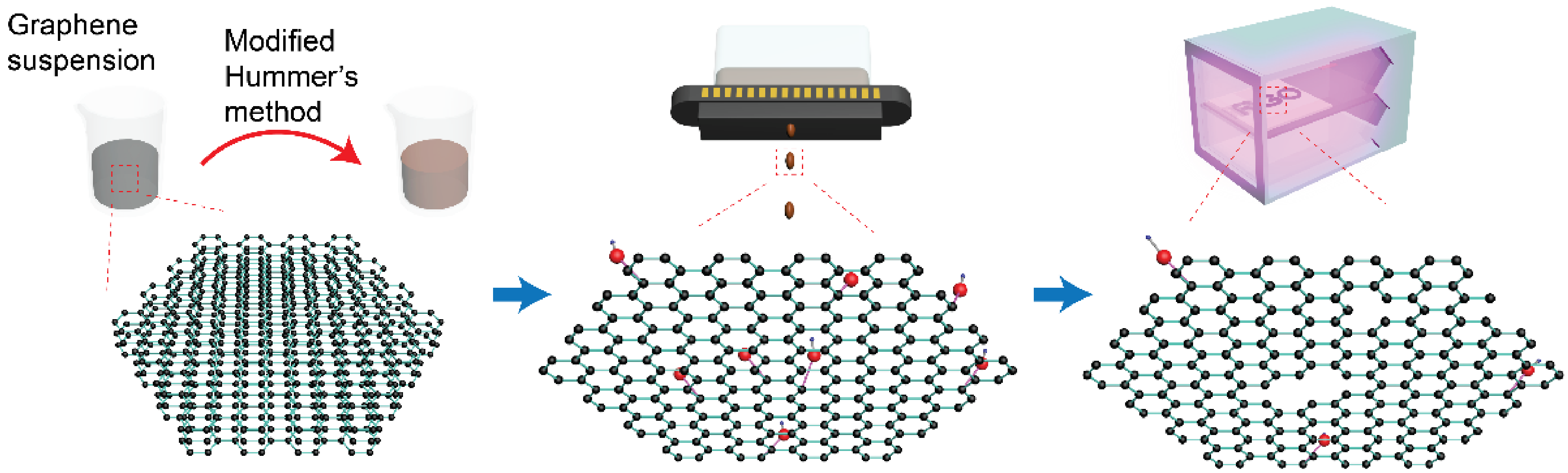

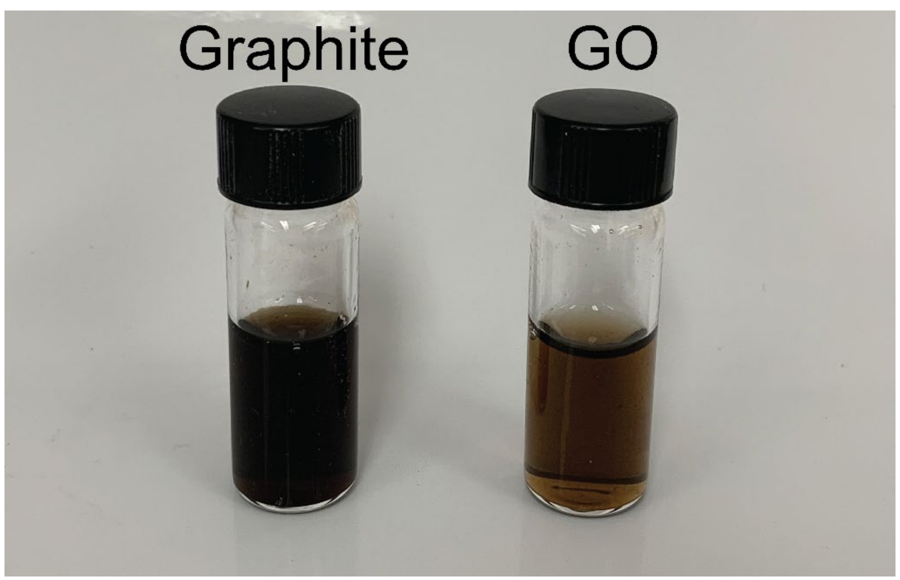

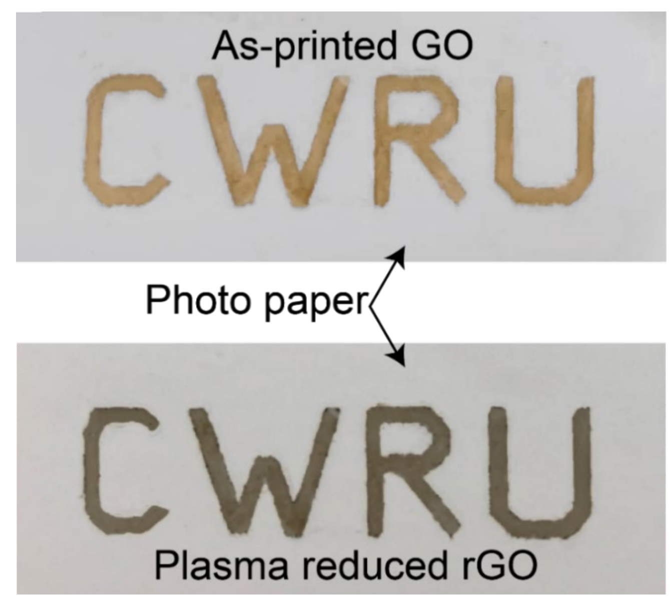

Adv. Mater. Technol. **4**, 1900834 (2019).

Characterization of plasma-converted rGO

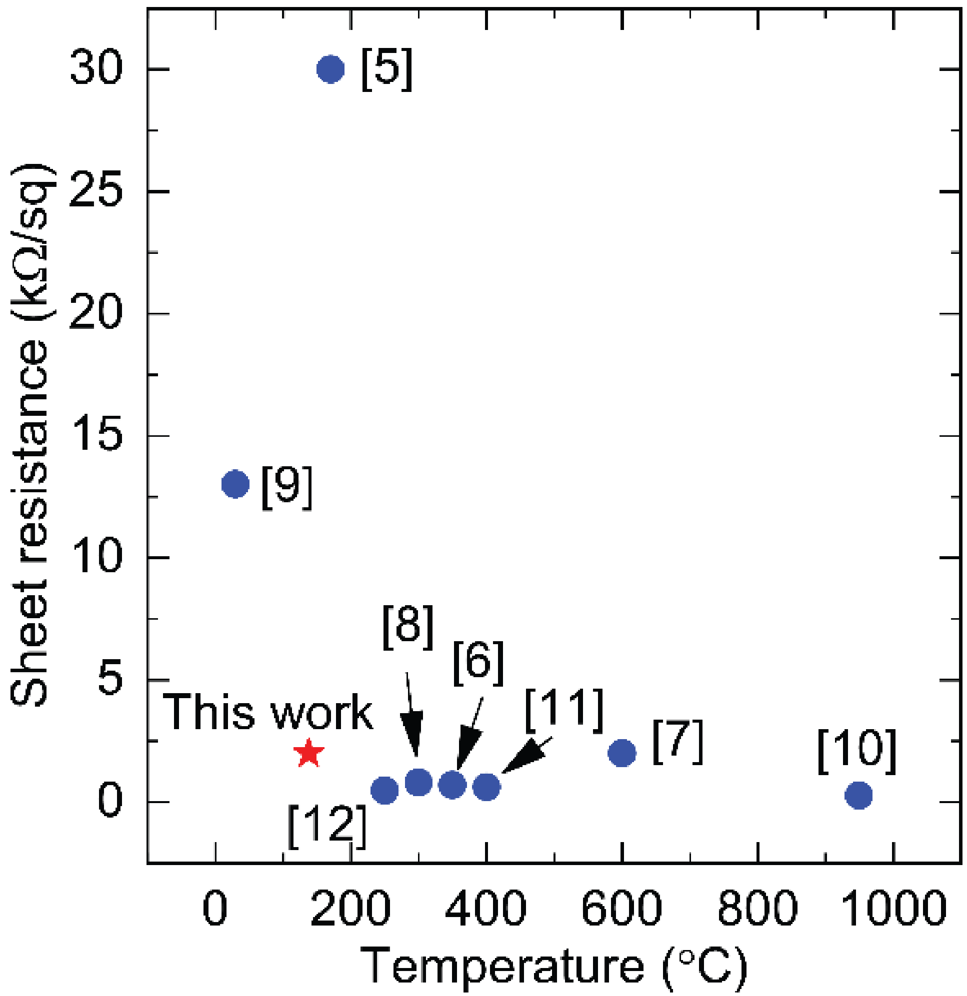

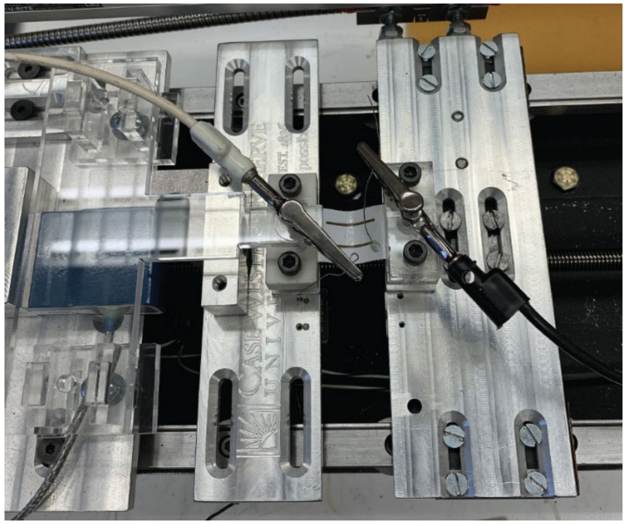

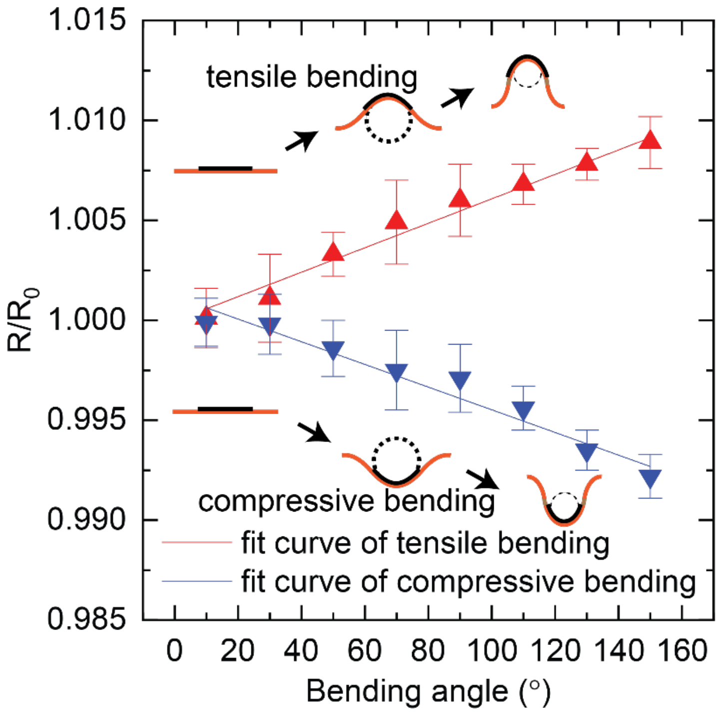

Adv. Mater. Technol. **4**, 1900834 (2019).

Atmospheric-pressure dielectric barrier (DBD) reactor with cold wall substrate heater

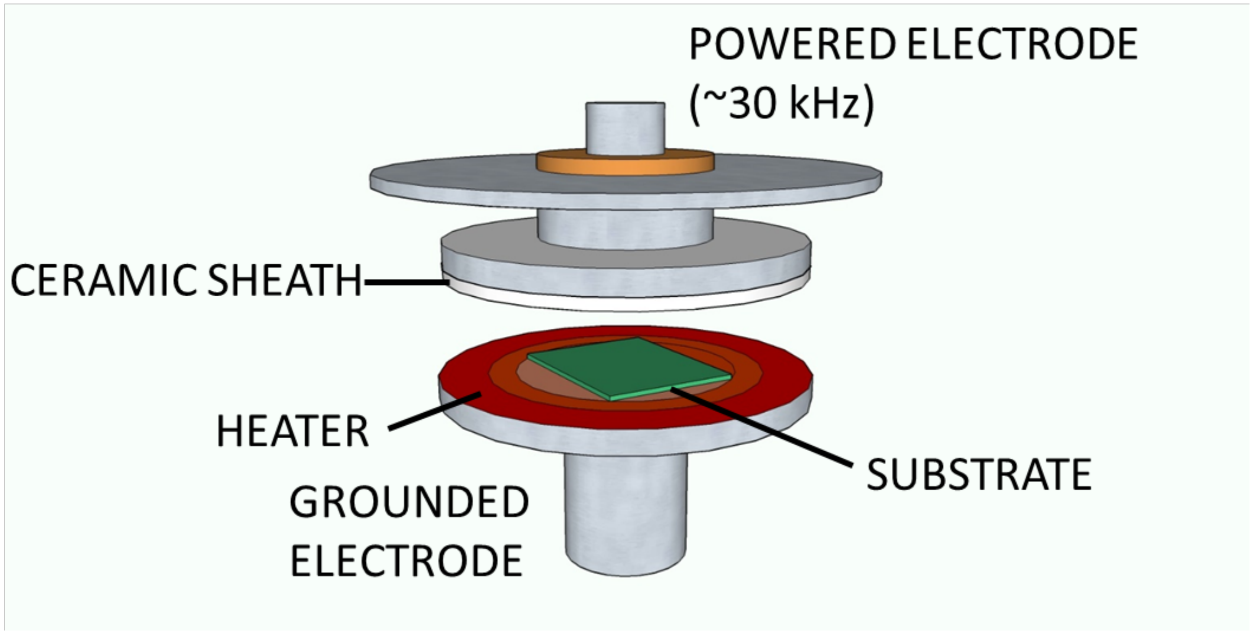

Electrode gap

6 mm

5 mm

4 mm

3 mm

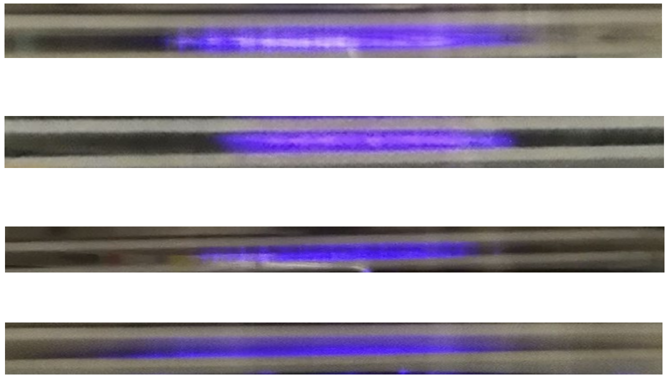

Plasma conversion of spin-coated ammonia borane to h-BN thin films (Ar only)

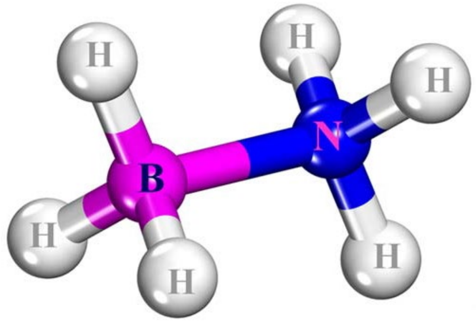

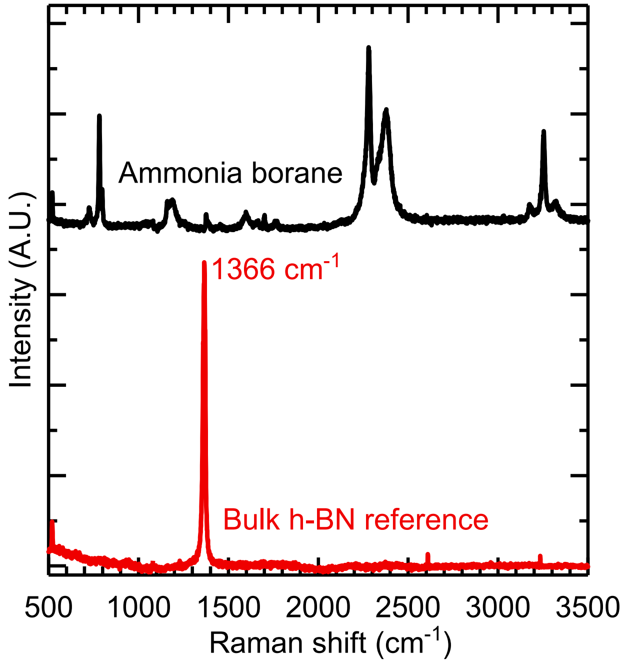

Micro Raman spectroscopy:

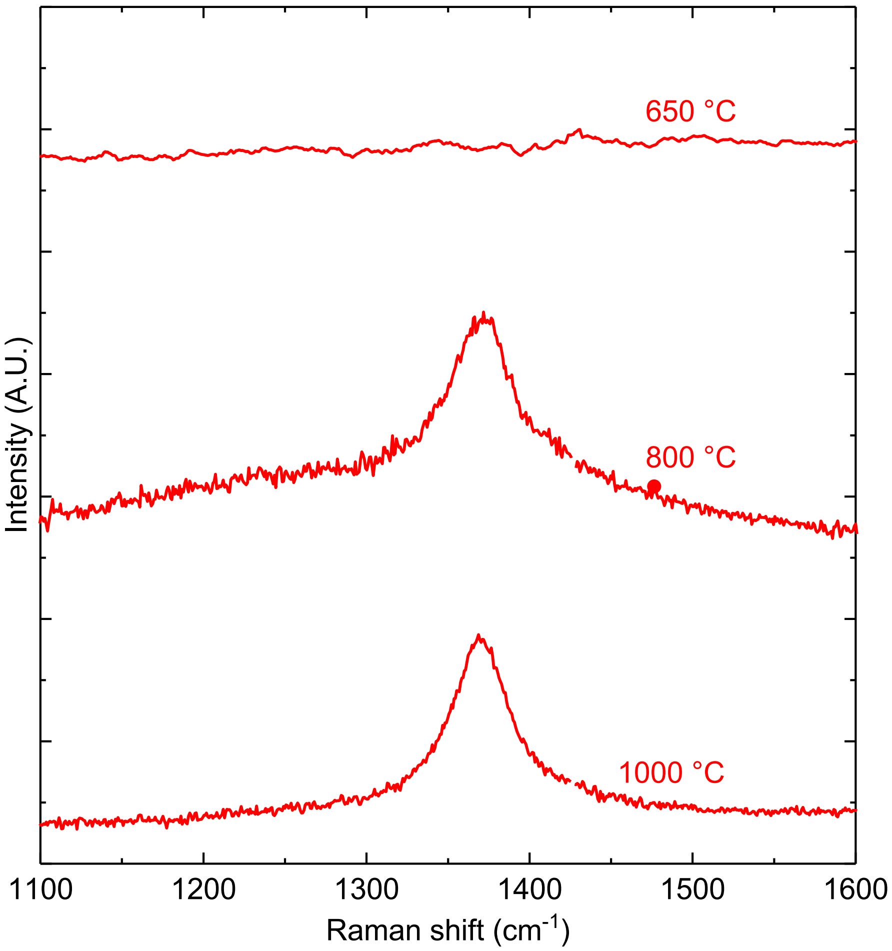

ACS Appl. Mater. Inter. **10**, 43936 (2018).

Plasma conversion of spin-coated ammonia borane to h-BN thin films (Ar only)

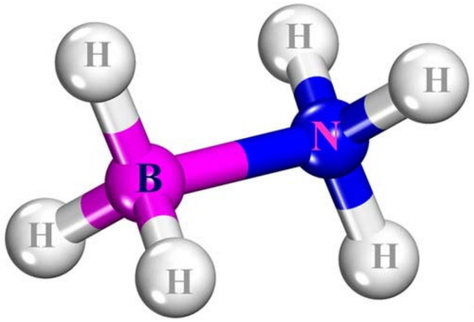

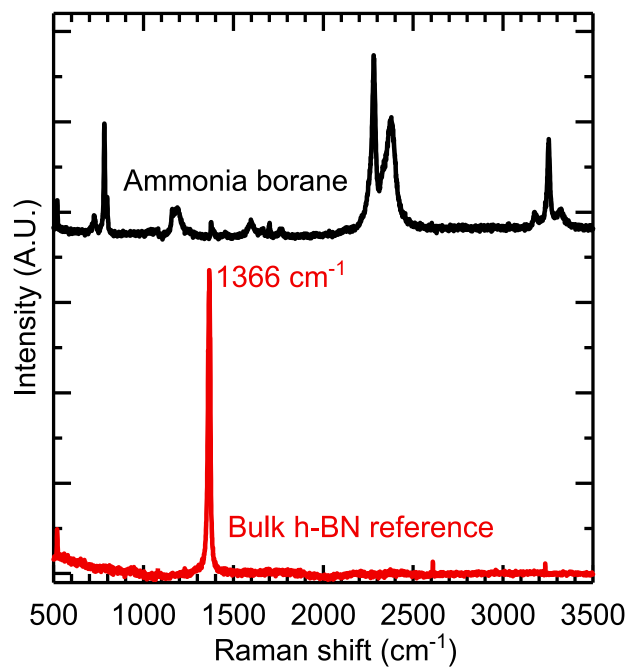

Micro Raman spectroscopy:

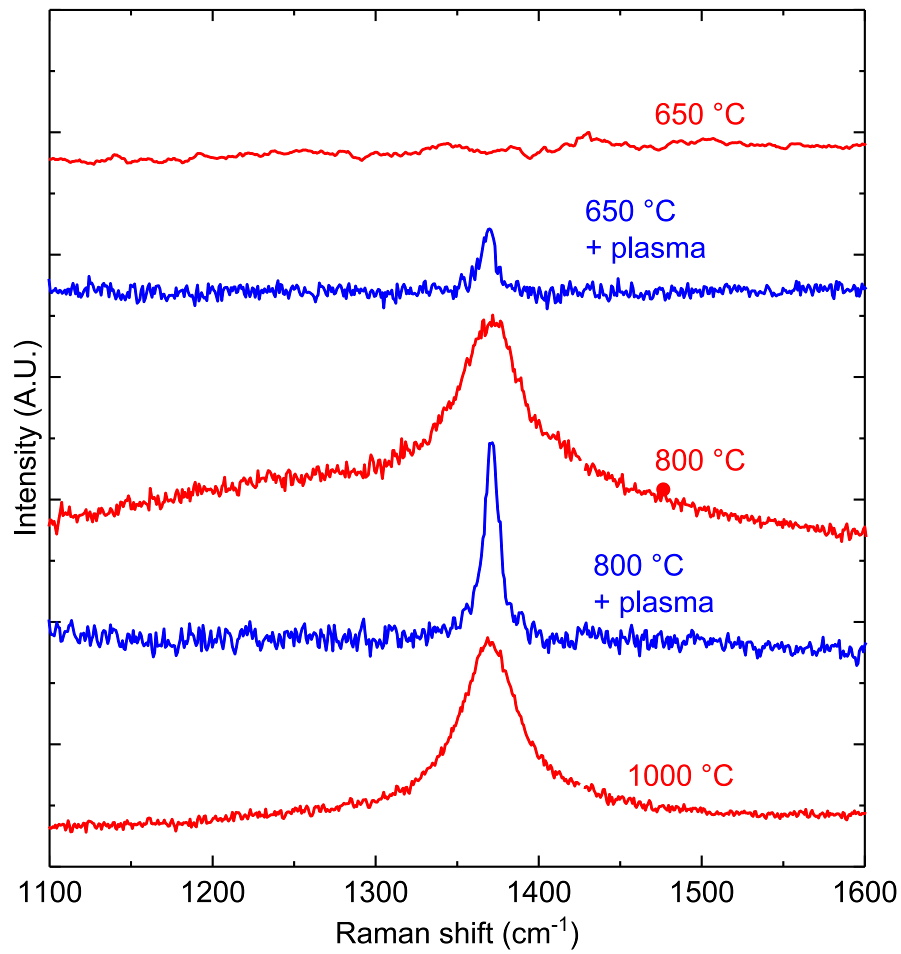

ACS Appl. Mater. Inter. **10**, 43936 (2018).

Plasma conversion of spin-coated ammonia borane to h-BN thin films (Ar + H_2)

Micro Raman spectroscopy:

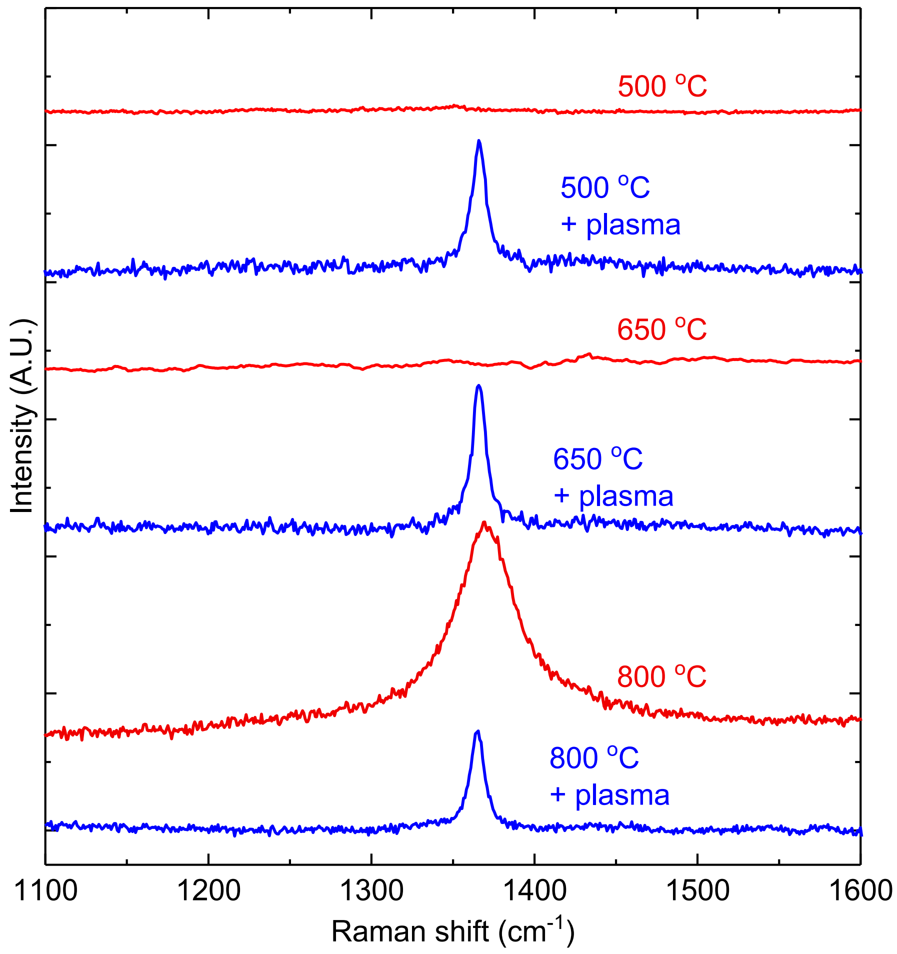

ACS Appl. Mater. Inter. **10**, 43936 (2018).

Assessment of film crystallinity by Raman analysis

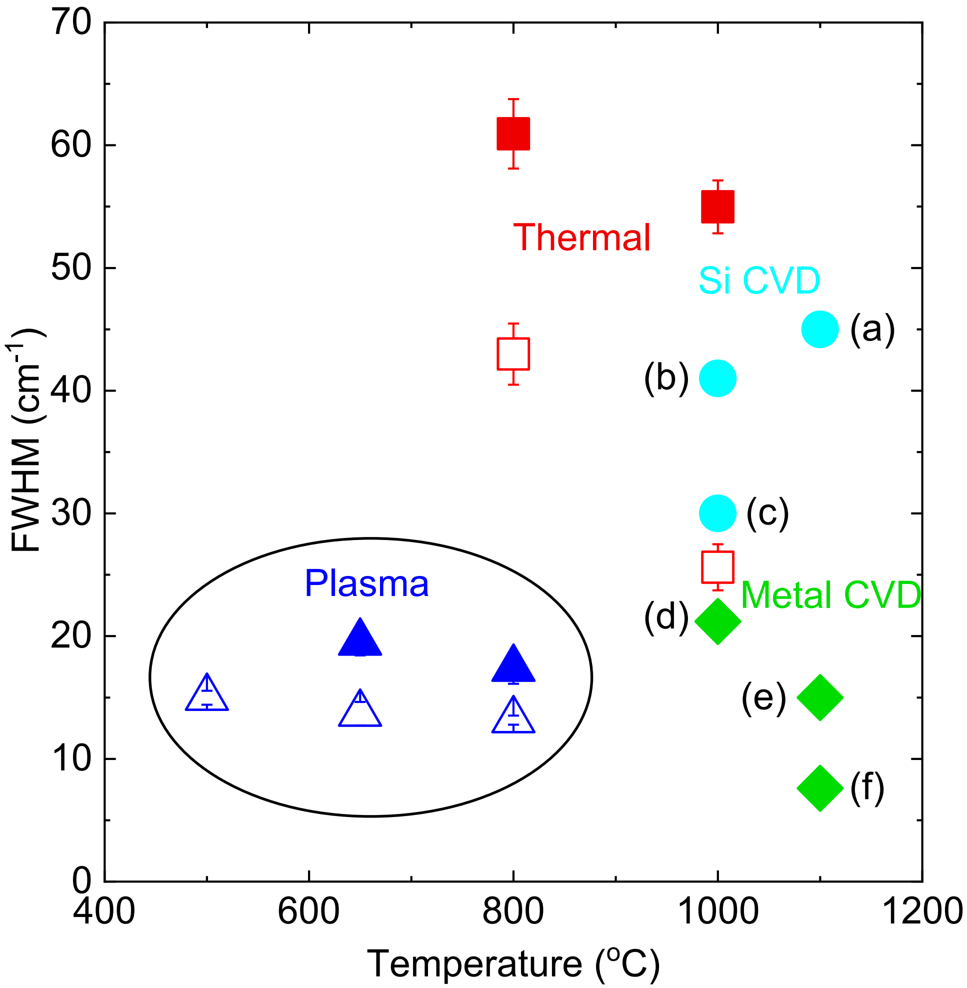

FWHM ($\Gamma_{1/2}$) is inversely rated to crystalline domain size (L_a):

$$L_a = \frac{1417}{\Gamma_{1/2}} - 8.7^*$$

*R. Nemanich *et al.*, *Phys. Rev. B* **23**, 6348 (1981).

(a)S. Behura *et al.*, *J. Am. Chem. Soc.* **137**, 13060 (2015).
(b)S. Behura *et al.*, *ACS Nano* **11**, 4985 (2017).
(c)R. Y. Tay *et al.*, *Appl. Phys. Lett.* **106**, 101901 (2015).
(d)L. Song *et al.*, *Nano Lett.* **10**, 3209 (2010).
(e)J-H. Park *et al.*, *ACS Nano* **8**, 8520 (2014).
(f) S. M. Kim *et al.*, *Nat. Comm.* **6**, 8862 (2015).

Proposed mechanism for plasma-enhanced chemical film conversion (PECFC)

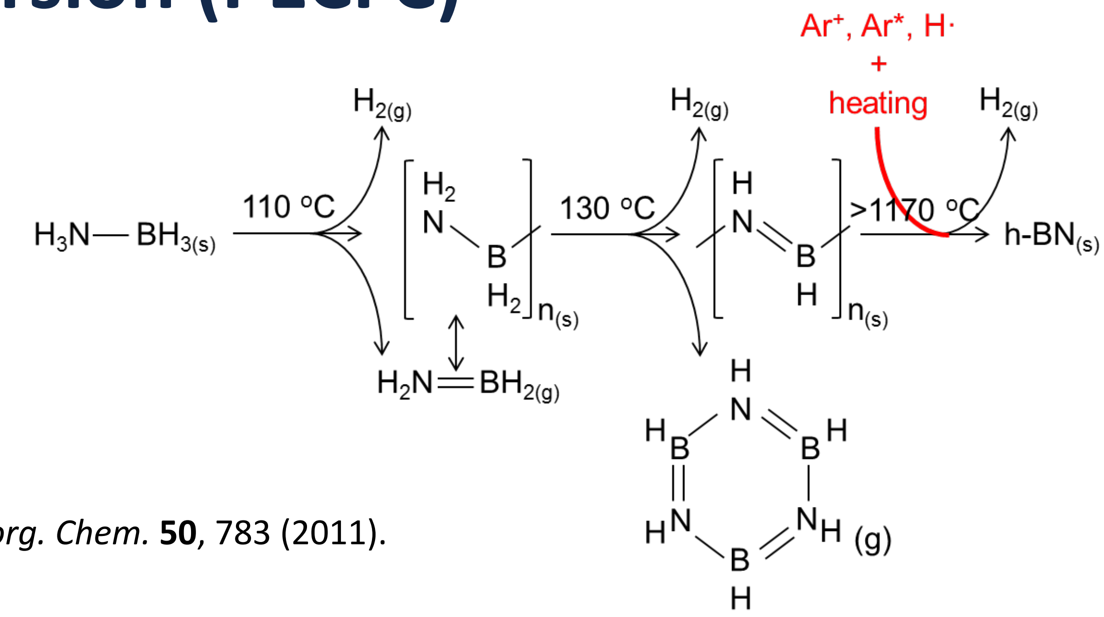

S. Frueh *et al.*, *Inorg. Chem.* **50**, 783 (2011).

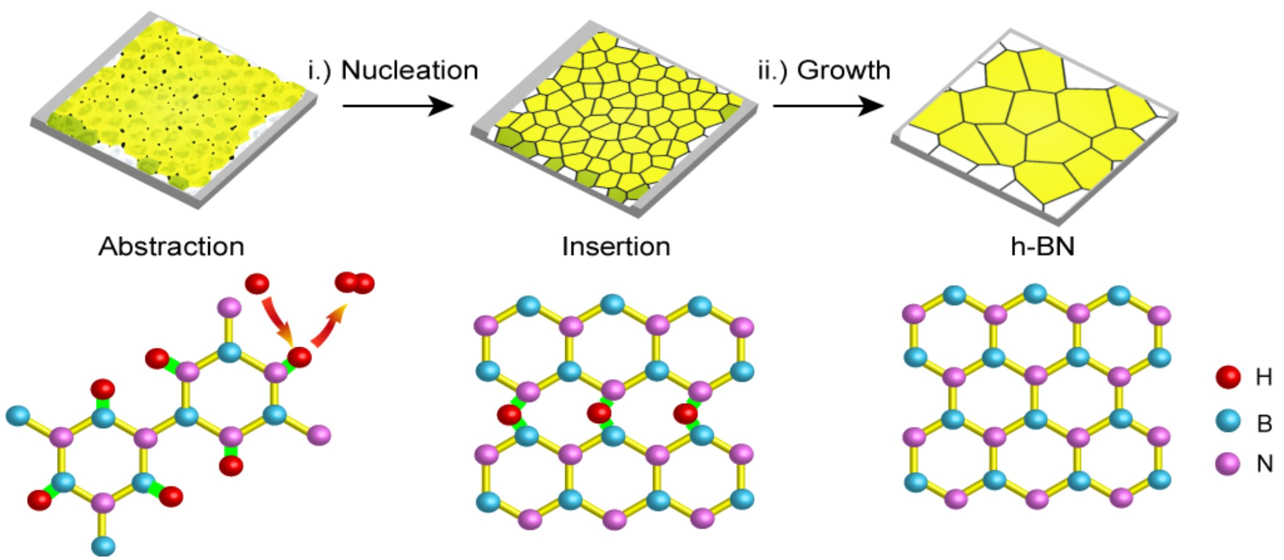

S. Sriraman *et al.*, *Nature* **418**, 62 (2002).
J. C. Angus *et al.*, *Science* **241**, 913 (1988).

Proposed mechanism for plasma-enhanced chemical film conversion (PECFC)

S. Frueh *et al.*, *Inorg*

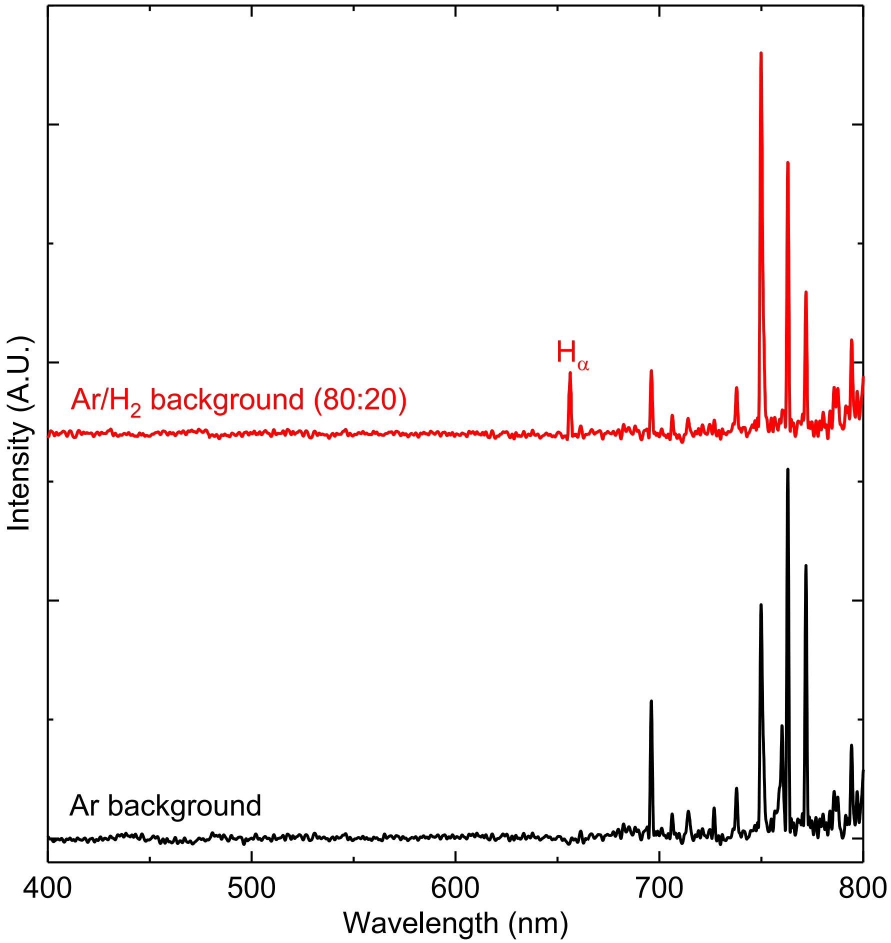

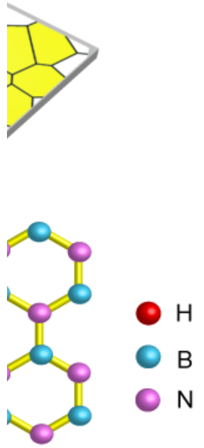

ACS Appl. Mater. Inter. **10**, 43936 (2018).

Demonstration of h-BN films as gate dielectric in 2D device

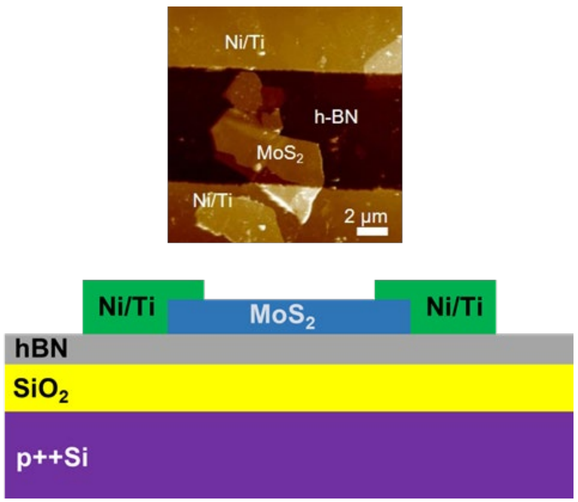

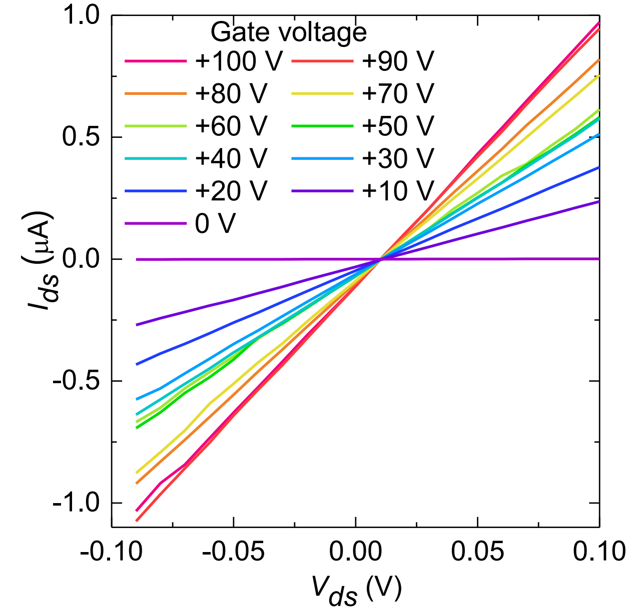

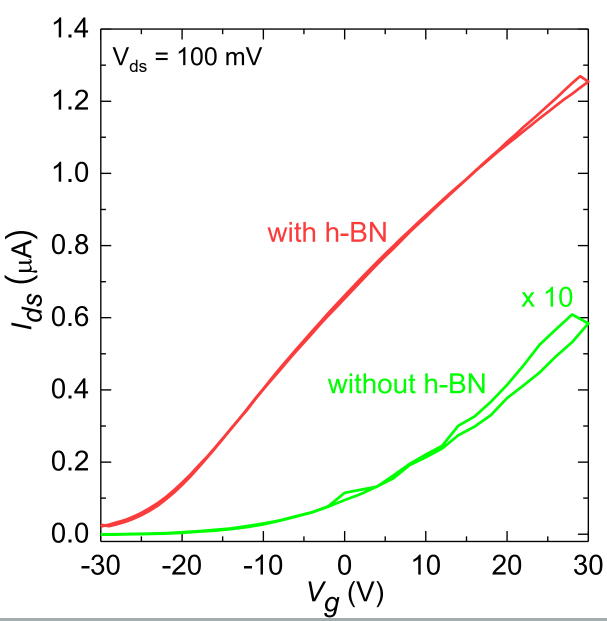

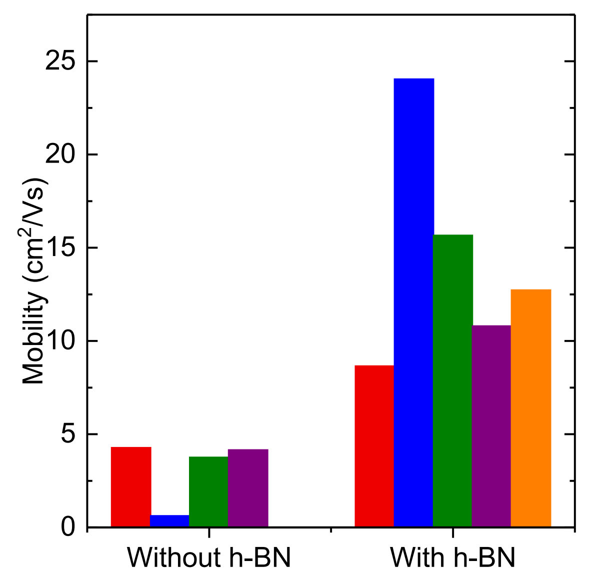

ACS Appl. Mater. Inter. **10**, 43936 (2018).

Extending PECFC to other layered materials: MoS_2 from $(NH_4)_2^{2+}MoS_4^{2-}$ (ATM)

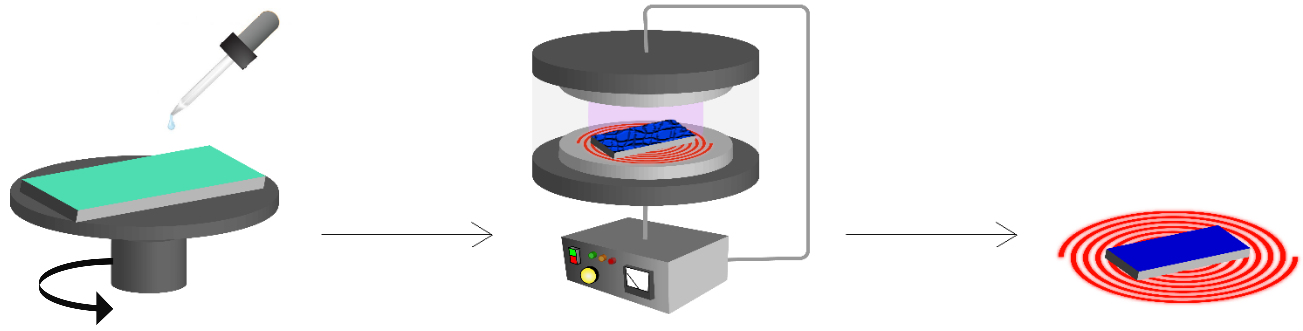

Spin-coated precursor film | Plasma-enhanced conversion step | High temperature annealing

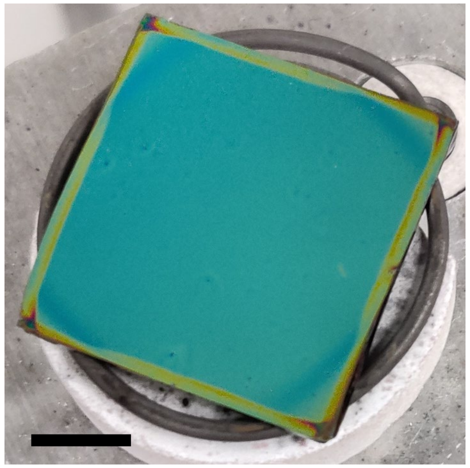

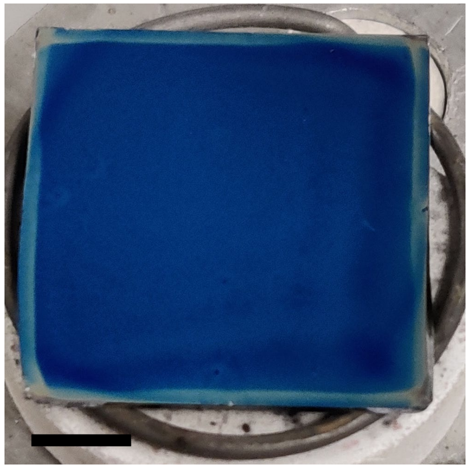

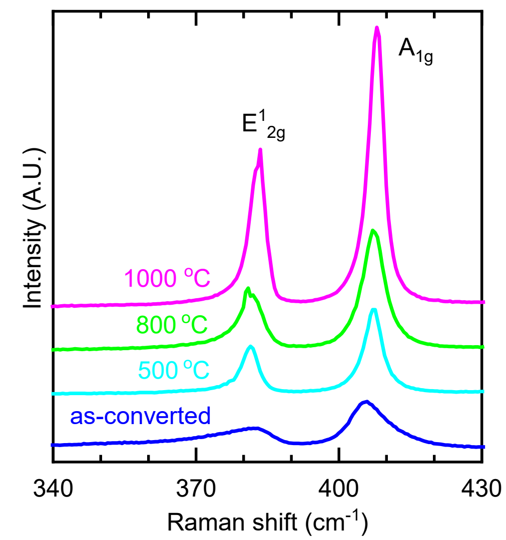

J. Vac. Sci. Technol. **38**, 063006 (2020).

Plasma *induces* nucleation, growth, and crystallization

Micro Raman spectroscopy:

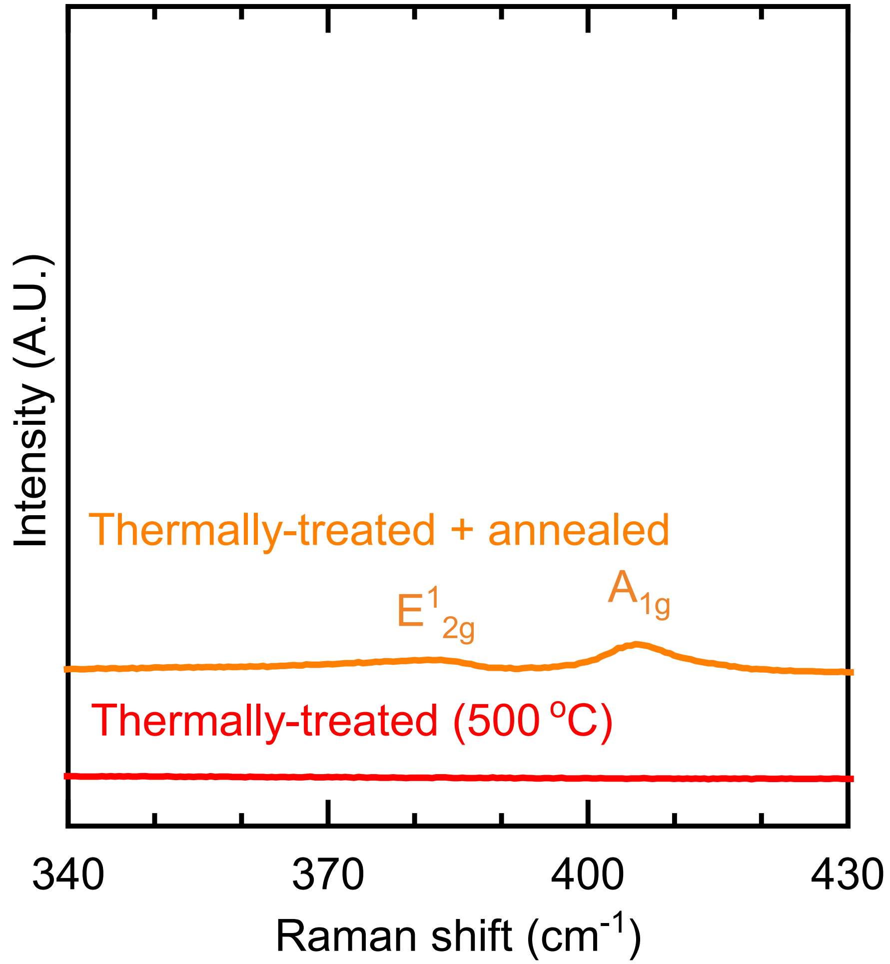

J. Vac. Sci. Technol. **38**, 063006 (2020).

Plasma *induces* nucleation, growth, and crystallization

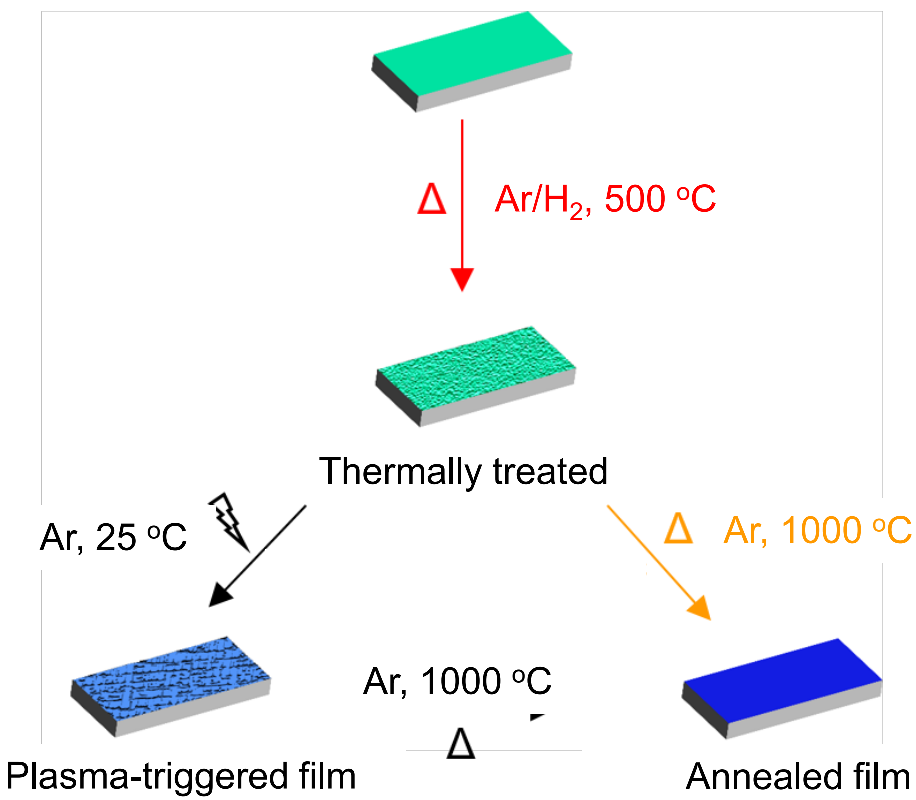

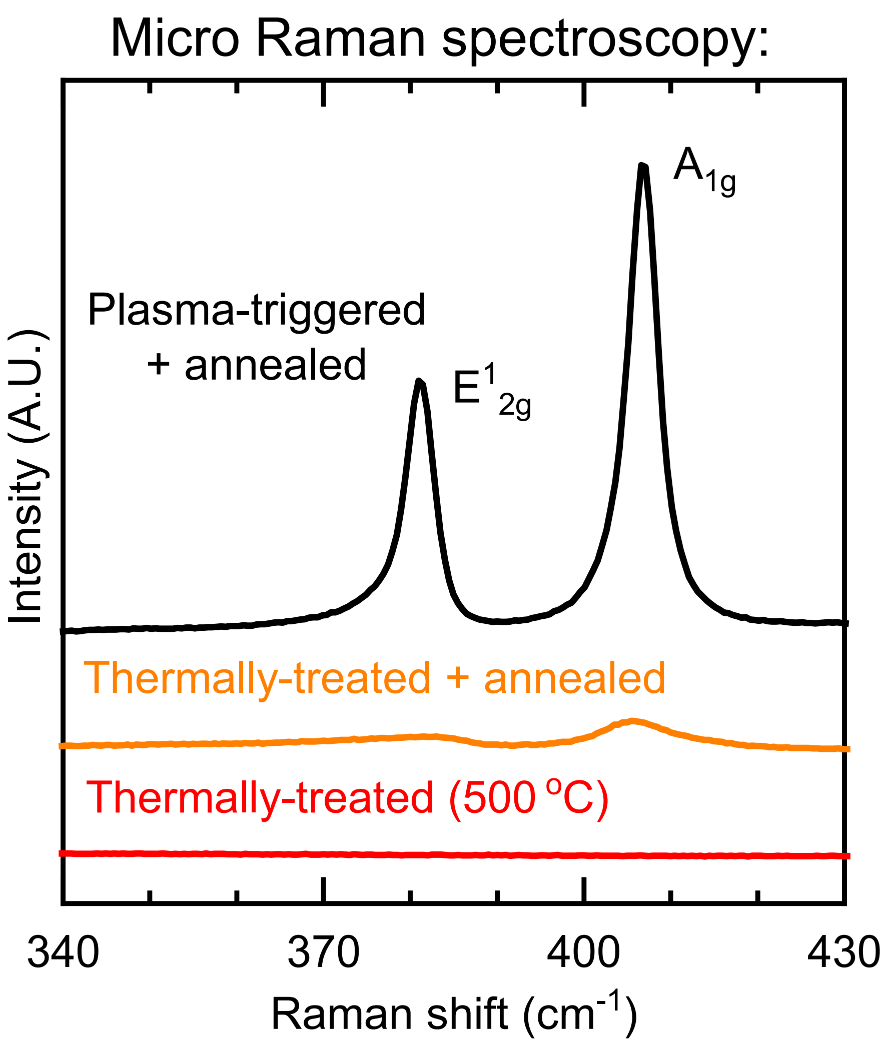

J. Vac. Sci. Technol. **38**, 063006 (2020).

Strain generation in MoS_2 films

Micro Raman spectroscopy:

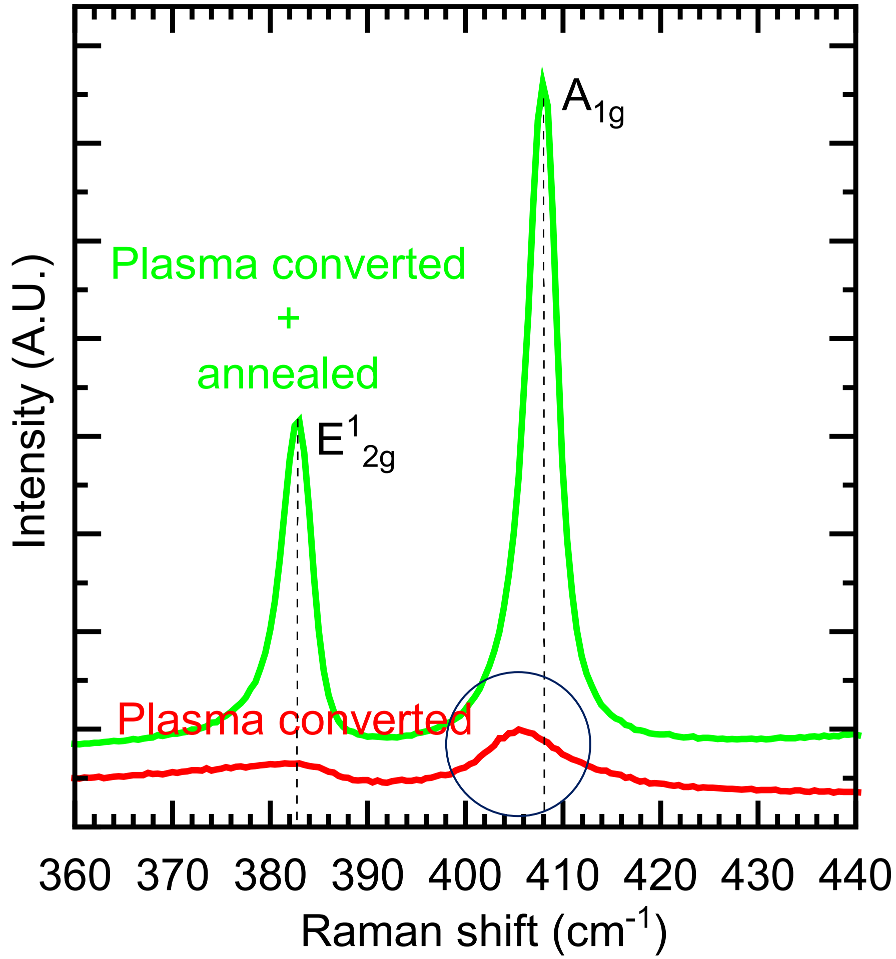

X-ray photoelectron spectroscopy:

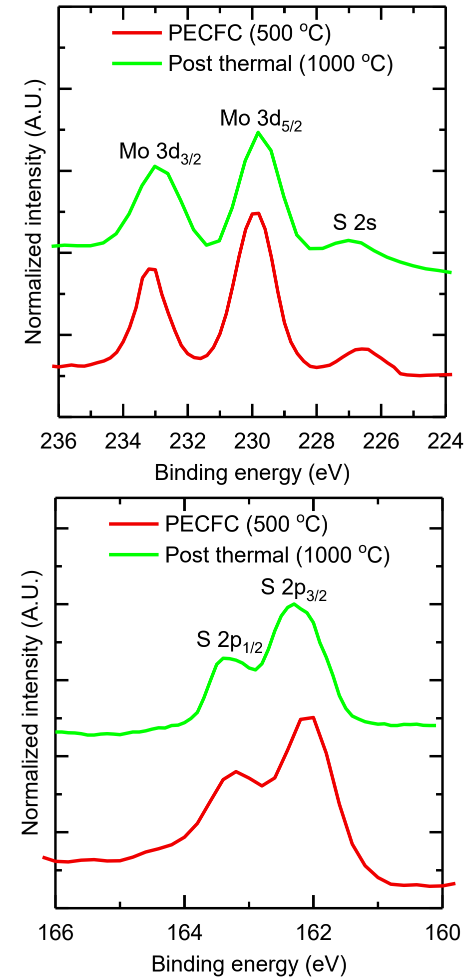

S:Mo ratio is constant!

ACS Appl. Energy Mater. **2**, 5163 (2019).

Types of defects in MoS_2

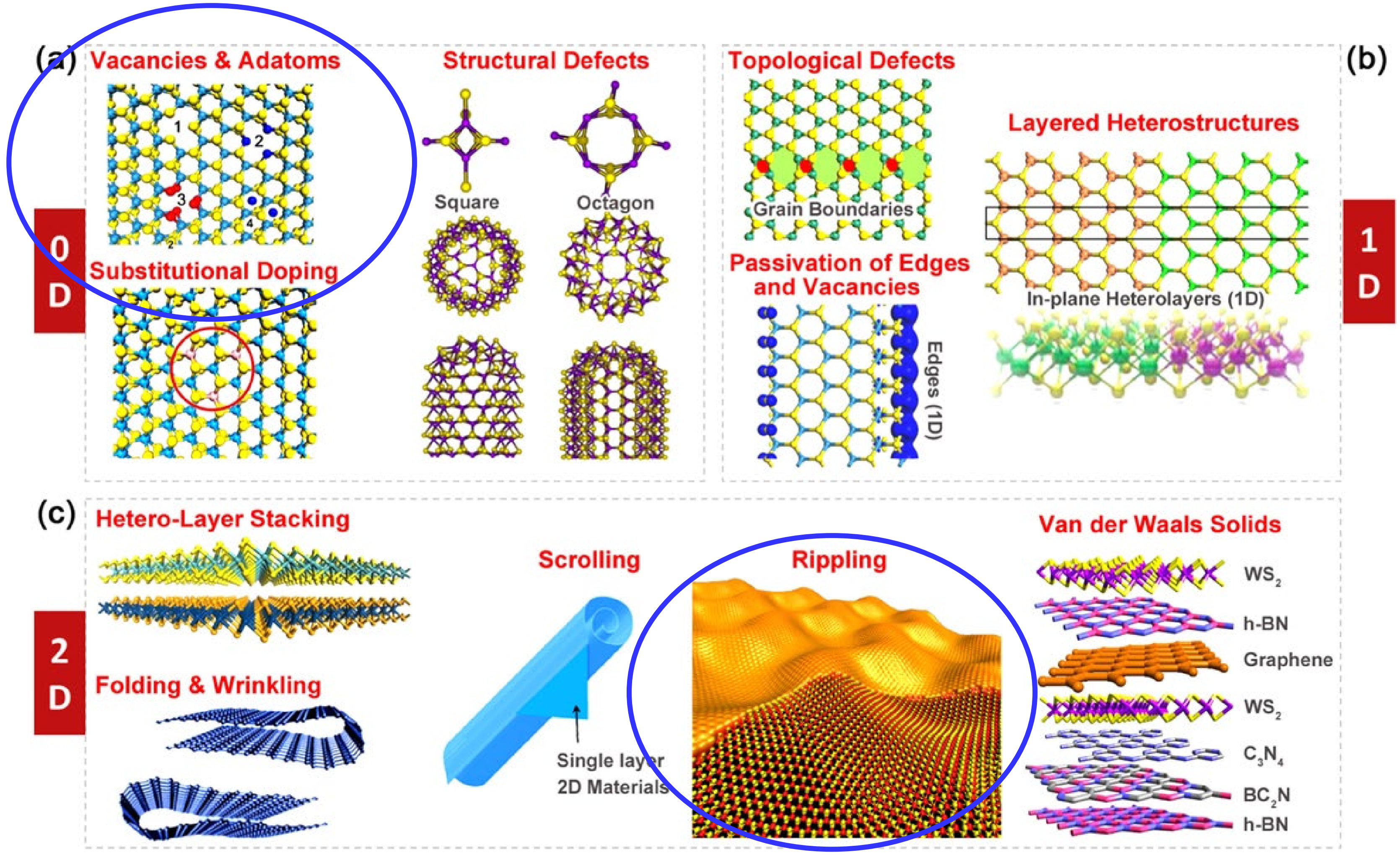

AFM characterization of plasma converted MoS_2 films: evidence for rippling

PECFC (500 ^oC)

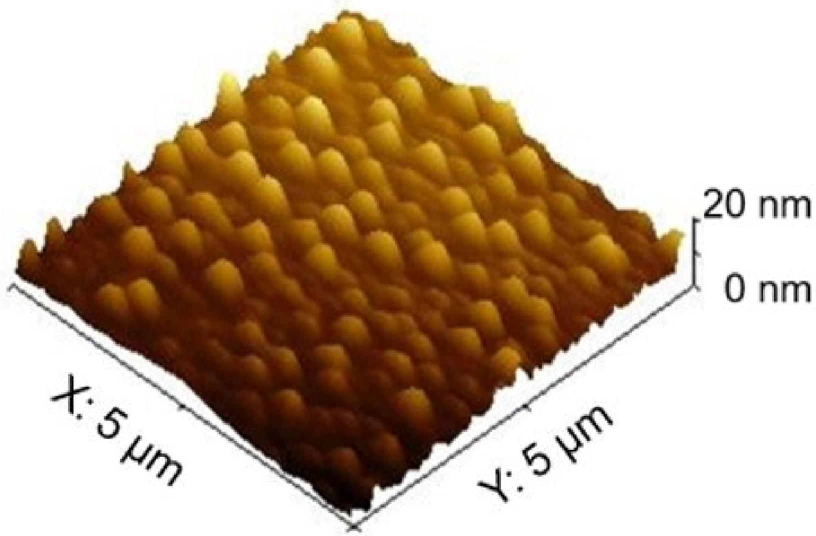

RMS roughness: 1.7 nm

Annealed (1000 ^oC)

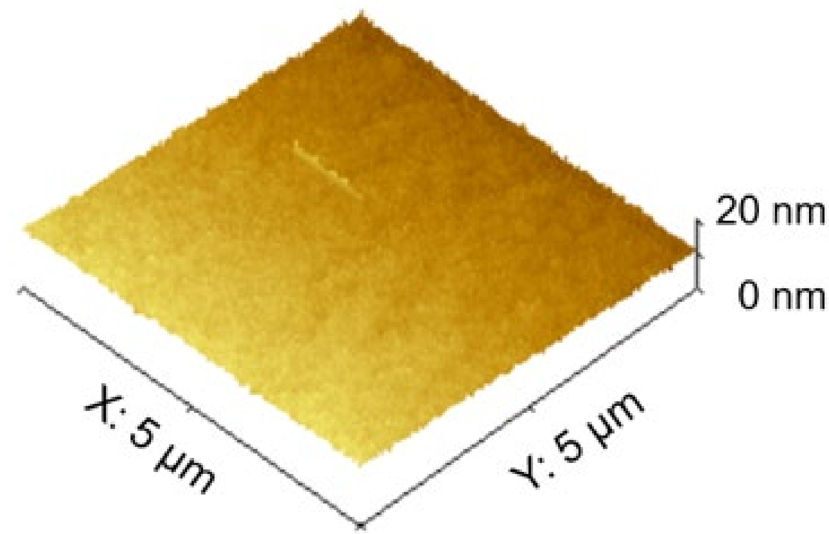

RMS roughness: 0.5 nm

ACS Appl. Energy Mater. **2**, 5163 (2019).

Plasma converted MoS_2 as catalyst for hydrogen evolution reaction (HER)

Polarization curves in 0.5 M H_2SO_4:

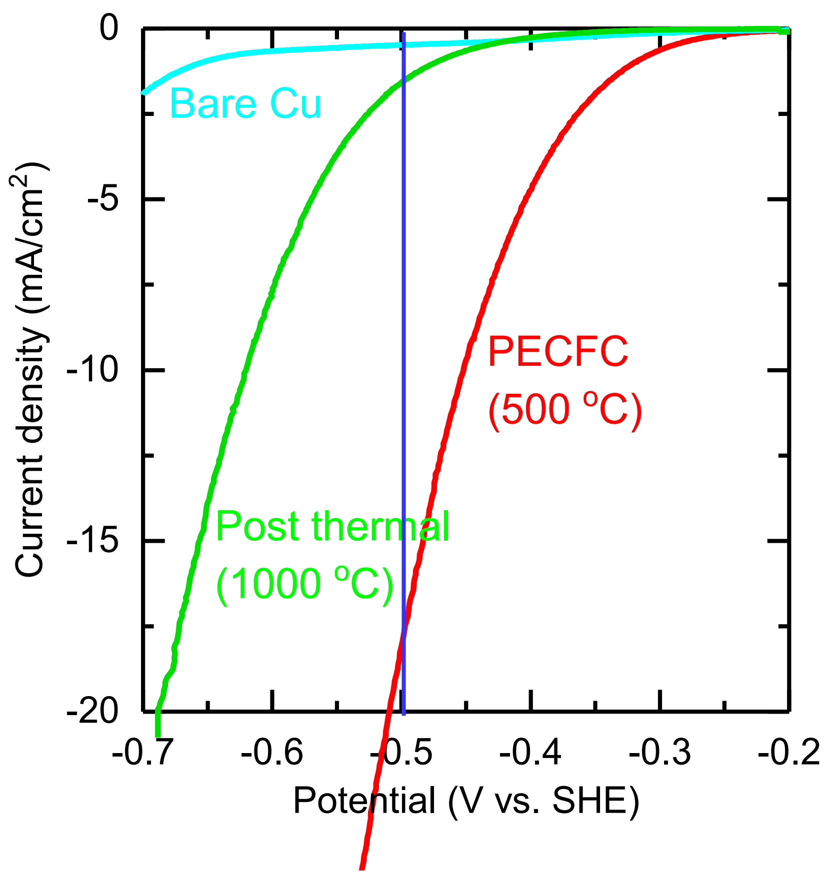

Double layer capacitance:

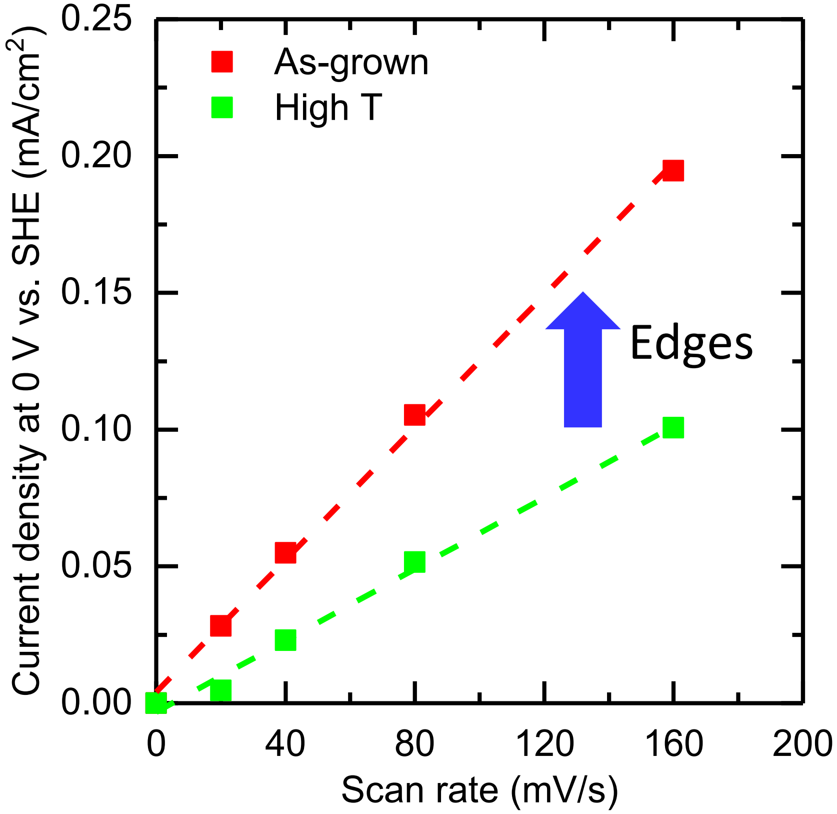

ACS Appl. Energy Mater. **2**, 5163 (2019).

Plasma converted MoS_2 as catalyst for hydrogen evolution reaction (HER)

Polarization curves in 0.5 M H_2SO_4:

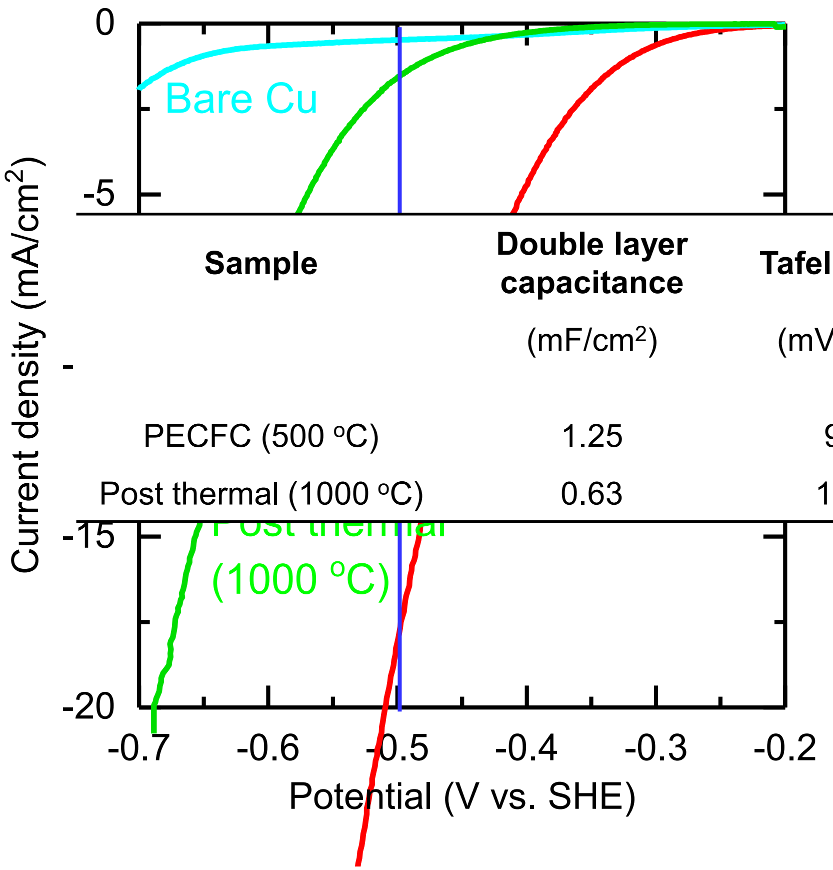

Double layer capacitance:

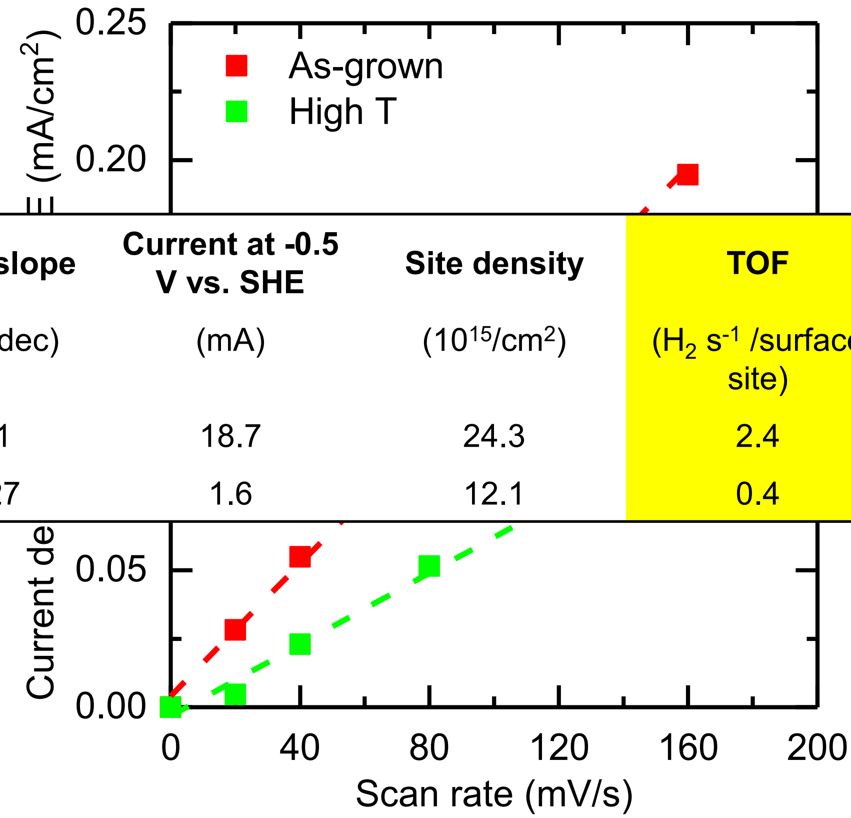

Sample	**Double layer capacitance** (mF/cm^2)	**Tafel slope** (mV/dec)	**Current at -0.5 V vs. SHE** (mA)	**Site density** (10^{15}/cm^2)	**TOF** (H_2 s^{-1} /surface site)
PECFC (500 °C)	1.25	91	18.7	24.3	2.4
Post thermal (1000 °C)	0.63	127	1.6	12.1	0.4

ACS Appl. Energy Mater. **2**, 5163 (2019).

Take home messages

Unique features of plasmas for AM:

- Ability to *chemically* convert, not just heat/sinter
- Gas-phase species for nucleation/growth and crystallization
- Charged species for low-temperature dissociation, electric migration, and defect generation

Challenges to overcome for AM:

- Lower processing temperatures even further for materials beyond metals
- Decrease resolution for direct write
- Integrate with existing tools for 3D fabrication

Acknowledgements

Alumni

- Carolyn Richmonds (Ph.D. candidate, Northwestern University)
- Dr. Seung Whan Lee (NAFRI)
- Megan Witzke (Exxon Mobil, New Jersey)
- Brittany Bishop (Ph.D. candidate, University of Washington)
- Dr. Souvik Ghosh (Intel)
- Evan Ostrowski (Ph.D. candidate, Princeton University)
- **Dr. Tianqi Liu (Chinese Academy of Science)**
- Ryan Hawtof (Ph.D. candidate, MIT)

Current group members

- **Souvik Bhattacharya (Ph.D. candidate)**

Collaborators

CWRU

Chemical and Biomolecular Engineering:

- Craig Virnelson
- Prof. C.C. Liu
- Prof. Rohan Akolkar

Materials Science and Engineering:

- Dr. Amir Avishai
- Dr. Jonathan Cowen
- Dr. Danqi Wang

Electrical Engineering and Computer Science:

- **Dr. Yongkun Sui (University of Colorado Boulder)**
- **Prof. Christian Zorman**

Funding: